Shaftless Screw Conveyors (Spiral Conveyors)

Collected Articles

by

Prof. Dr. Friedrich Krause and Dr. Andrey Minkin

Otto-von-Guericke University of Magdeburg,

Faculty of Mechanical Engineering,

Chair of Material Handling (IFSL),

39106 Magdeburg, Universitaetsplatz 2, Germany

2005

Библиографическое описание и краткий реферат

Название: „Винтовые ковейеры без вала“, Сборник статей

Автор: Проф. Ф. Краузе, к.т.н. А. Минькин, Отто-фон-Герике Университет Магдебург, Факультет машиностроения

Краткий реферат:
Винтовые конвейеры без вала (известны также как Спиральные конвейеры) применяются для транспортировки таких сыпучих грузов, для которых обычный Винтовой конвейер не может быть использован.

Так как Винтовые конвейеры без вала сильно отличаются от обычных Винтовых конвейеров, то существующая методика расчета и конструирования Винтовых конвейеров не может быть использована для расчета и конструирования Винтовых конвейеров без вала.

В настоящем сборнике статей приведено описание экспериментальных и теоретических исследований для Винтовых конвейеров без вала. Для решения задачи экпериментальных исследований были построены две испытательные установки, оснащенные измерительной техникой.

Основываясь на результатах экспериментальных и теоретических исследований была разработана и представленна методика расчета и конструирования Винтовых конвейеров без вала.

Ключевые слова: Винтовой конвейер без вала, Спиральный конвейер, Винтовой конвейер, Машины непрерывного транспорта, Механика сыпучих грузов.

Bibliographical Description and Abstract

Title: “Shaftless Screw Conveyors“, Collected Articles

Author: Prof. Dr. F. Krause, Dr. A. Minkin, Otto-von-Guericke University Magdeburg, Faculty of Mechanical Engineering

Abstract:
The shaftless screw conveyors (also known as spiral conveyors) are used in those cases, when the usual screw conveyors cannot be used.

The principles of calculation for screw conveyors cannot be applied for shaftless screw conveyors, because of their considerable differences.

Here the theoretical and experimental investigations of shaftless screw conveyors are presented. With this purpose, two pilot plants equipped with measuring technology were built.

Based on extensive results of theoretical and experimental investigation the scientific principles for the calculation and design of shaftless screw conveyors were developed.

Keywords: Shaftless Screw Conveyor, Spiral Conveyor, Screw Conveyor without Shaft, Bulk Solid Handling.

Index

Research on shaftless screw conveyors 2

Theoretical and experimental study of horizontal and lightly inclined shaftless screw conveyors. Part 1 17

Theoretical and experimental study of horizontal and lightly inclined shaftless screw conveyors. Part 2 28

Nomenclature 42

Literature 44

Research on shaftless screw conveyors

Abstract

This paper is concerned with the shaftless screw conveyors (SSCs), also known as "spiral conveyors" and describes some important distinctive features in contrast to the usual screw conveyors (SCs). The paper focuses on qualitative study of SSCs.

1 Introduction

The principle of screw conveyance has a special significance in bulk solids handling technology. It has been used since antiquity. This principle can be used for a wide spectrum of bulk solids (from powder to fine-grained) and allows horizontal, inclined and vertical lines of transportation and a wide variation in the throughput according to need. In addition, the bulk solid in the conveyor is insulated from the environment by the trough.

The SSCs (Fig.1, l.) open up new and special areas of application for screw conveyance, which are determined according to the special properties of the bulk solids.

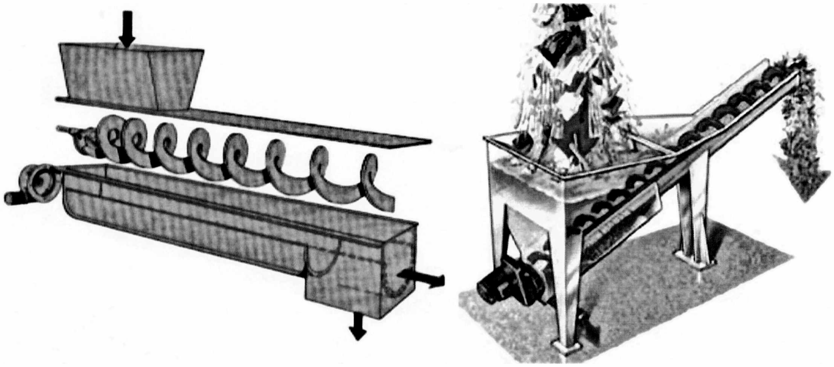

Fig 1: Design of horizontal SSC (HSSC) (l.) and SPIRAC-Dewaterer (r.) (Source: SPIRAC)

The SSCs are used in those cases, when the usual SCs cannot be used. Hence the application field of SCs is expanded by the SSCs.

The SSC are used in the transport of cohesive, adhesive, semisolid, paste, fibered bulk solids and solid-water mixtures (Fig 1, r.). The SSCs are mainly used in sewer plants and plants for dust, tree, pulp, paper and food processing, agriculture and building industry.

The SSCs have been known for a long time, but only after 1975, industries started developing and manufacturing of them. Although screw conveyors have been completely investigated [1], [4] – [8], [15], [19] – [22] beginning in 1957, consecutive research on SSCs has not yet been conducted. Today, in the most companies the design of the SSCs is based only on the practical experience. Absence of scientific principles for the design of SSCs was the reason for this study.

2 Design and principle of work

The SSCs consists of a shaftless screw, which is supported by a wear-resistant liner attached to the inside surface of the trough and is insulated from the environment. The shaftless screw revolves on its axis and pushes or pulls the bulk solid in the axial direction. In this context one should distinguish between the "pushed" and "pulled" SSC-systems. The "pulled" SSC-systems are applied for inhomogeneous bulk solids with high density. The "pushed" SSC-systems are used for fibered bulk solids to avoid the mortise dowel joints in the field of drive [7], [14], [24].

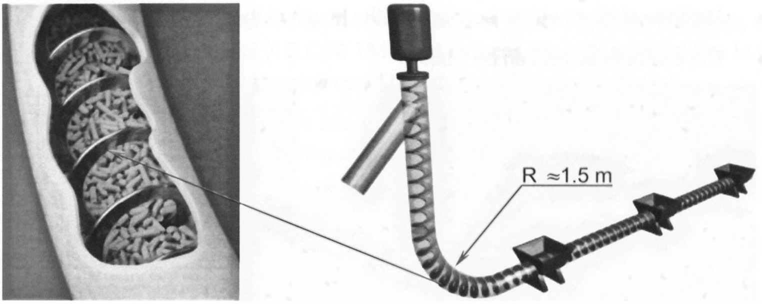

Fig 2: The flexible SSC for the transportation of the wood pellets (Source: Company Steiner from Simbach)

The SSC has a maximum length of 60 … 80 m and works without intermediate bearings on the conveyor line. The trough of the SSCs is U-shaped or O-shaped and equipped with a wear-resistant liner (in the case of HSSCs). The shaftless screw consists of one to three helical flights. The number of flights depends on the bulk solid properties, angle of elevation and length of conveyor.

The SSCs can have the flexible and inflexible shaftless screw. In this context the SSCs can be divided into two groups: flexible and inflexible shaftless screw conveyors. In contrast to the inflexible shaftless screw conveyors and usual screw conveyors the use of flexible shaftless screws makes curved lines of transportation possible (Fig. 2). In this study, the inflexible SSCs are only considered.

For the manufacture of shaftless screws, troughs and wear-resistant liners depending on bulk solid properties and case of application, the different materials including the usual constructional steels (St 52-3, St 60) and alloyed steels (chrome- or manganese-based steels like X5 CrNi 1810), plastics (wear-resistant high-molecular polyethylene, PA, PE, PU, PP, and other) may be used. The shaftless screw may be galvanized or plastic-coated (max. 1.5 mm with PA, PU, PVDF) to protect against the aggressive bulk solids.

The bulk solid's motion in the trough of SSC has a similar character as in the SC and based on widely known "screw and nut"-motion principle.

3 Distinguishing features of SSCs

In contrast to the usual SCs, SSCs show the following important distinctive features:

- **In design:**
  - The screw is without shaft ("spiral"),
  - The screw is mounted on the drive only,
  - The shaftless screw consists of one to three helical flights and is supported by the wear-resistant liner attached to the inside surface of the trough,
  - Absence of intermediate bearings on the length of the conveyor line,
  - The shaftless screw can be flexible.

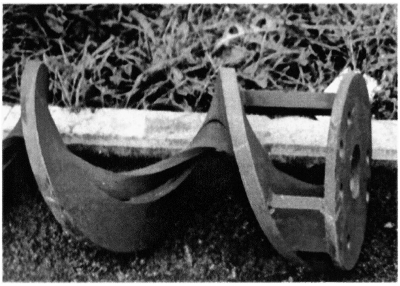

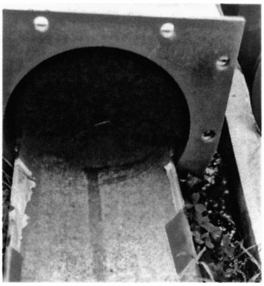

Fig. 3: Shaftless screw, U-shaped polyethylene wear-resistant liner (Source: DIM GmbH, ImRo Bückeburg)

- **In principle of work:**
  - The shaftless screw of horizontal and inclined SSCs is supported by a trough,
  - There is no defined radial clearance, consequently almost no backflow between the shaftless screw and trough,
  - For the SSCs the higher fill ratios ($0.7 \leq \eta_F \leq 0.9$) are typical,
  - The SSCs work only with low rotational speeds, i.e. limited throughput. In the case of steeply inclined and vertical transportation lines, the principle of work is provided by very high fill ratios ($\eta_F \approx 1.0$) and continual feeding, and a shaftless screw consisting of three helical flights,
  - The bulk solid transportation is actuated by the form in field of shaftless screw flight and by internal friction in the field of shaftless screw core,
  - The unloading facility of the conveyor is possible not only in the radial direction as screw conveyors, but also in the axial, because the shaftless screw is fastened to the drive only,
  - The use of flexible shaftless screws makes curved lines possible [15], [23].

- **In areas of application:**
  - The absence of a shaft increases the trough area, which can be filled with bulk solid. The possibility of transportation of cohesive, fibered and heterogeneous bulk solids is better (Fig. 4),
  - The shaftless screw eliminates the need to clean the shaft. The transportation of the cohesive bulk solids is more efficient. Additionally, the transportation of bulk solids is realized without any emission or immission,
  - Fastened wear-resistant liner on the internal surface of the trough results in decreased trough abrasion and power consumption during the transport of abrasive bulk solids. The wear-resistant liner is made of metal or plastic materials, such as polythene or material X 5 CrNi 1810 and reduces the bulk solid caking. In particular cases the shaftless screw could be galvanized or plastic-coated,
  - *Shaftless screw conveyors are mainly used in sewer plants and plants for waste, tree, paper, food and building materials processing industry.*

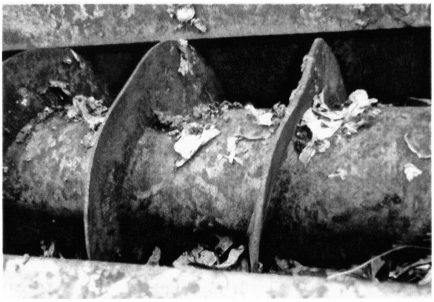

Fig. 4: The SC was replaced with SSC, because it didn't pass for transportation of the cut waste material

4 Design of the pilot plant and the test rig

With the purpose of investigating the character of the bulk solids motion in the trough, optimum velocity of transportation, motion resistance, drive capacity and volumetric (mass) throughput under variable conditions of bulk solids properties, fill ratio and rotational speed, the Institute for Conveyor Technology (IFSL) of Otto-von-Guericke University Magdeburg designed and built in cooperation with the company DIM GmbH from Dessau, the large-scale pilot plant and one model test rig equipped with measurement technique for experimental research.

4.1 Description of the pilot plant

Figure 5 shows the large-scale pilot plant and its components in the IFSL Lab.

HSSC

Manufacturer's characteristics:

n_{Wn} = 16.1 min^{-1}, η_{Fn} ≈0.7,

I_{Vn} ≈5.2 m^3/h (by k_F ≈0.8),

Length of trough: L_T = 3800 mm

U-section of trough (diameter/length):

d_{TU} = 260 mm, L_{T1} = 2795 mm

O-section of trough (diameter/length):

d_{TO} = 250 mm, L_{T2} = 1005 mm

Wear-resistant liner: X5 CrNi 18.10,

s_{Schl} = 10 mm, α_{Schl} = 130°,

Shaftless screw: two helical flights,

L_W = 3700 mm, l_{St} = 225 mm,

d_{W1a} = 233 mm, d_{W2a} = 117 mm

d_{W1i} = 117 mm, d_{W2i} = 29 mm

b_{W1} = 58 mm, b_{W2} = 44 mm

s_{W1} = 18 mm, s_{W2} = 13 mm

Drive: P_n = 4 kW,

n_W = 0.3 ... 27 min^{-1}, M_n = 2132 Nm

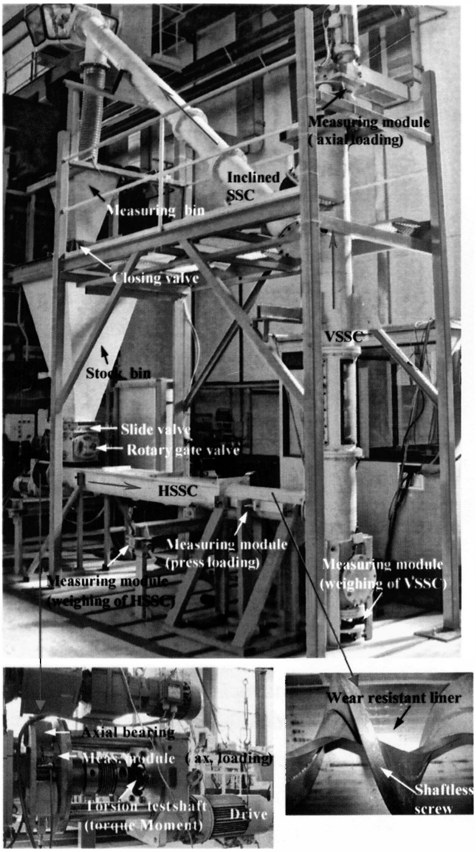

Fig. 5: The pilot plant and its components

The U-shaped section of HSSC-trough is connected to a 1-meter long O-shaped section at the intersection of the horizontal and vertical conveyors. Such design of HSSC-trough is necessary not only for joining of HSSC with VSSC, but also for decreasing of trough-diameter on the conveyor's length and consequently for increasing of fill ratio on the intersection between the two conveyors. Consequently, there is no backflow from VSSC into HSSC.

The system of measurement and storage of bulk solid is necessary to define mass throughput. The rotary gate valve equipped with a frequency regulator is used to regulate the fill ratio in the horizontal conveyor. Between the drive and shaftless screw of each of the SSCs are fastened three measuring modules (based on strain gauge technology), which determine axial force. Two measuring modules are mounted on the intersection between the horizontal and vertical conveyor to determine press loading. The HSSC is also mounted on four (three in the case of VSSC) measuring modules to determine their fill ratio.

All crossing points of HSSC and VSSC are supplied with rubber manifolds to facilitate the weighing of each conveyor and to determine press loading. It is possible to measure and adjust the driving speed through a frequency regulator connected to each of the drives. For the horizontal conveyor of the pilot plant, the torsion test shaft is mounted between the drive and shaftless screw. The torsion test shaft enables the measurement of the total torque. The horizontal and vertical conveyors are supplied with windows for observation of the bulk solid's motion character.

The analog signals of the experiments are transmitted to the analog/digital card in computer, where they are digitalized and transmitted to the DIADEM software ("Measured signal → amplifier → 16 channel measuring analog/digital card → Software DIADEM").

4.2 Description of the test rig

Figure 6 shows the model test rig and its components, which was built by IFSL in cooperation with DIM GmbH and Wildfellner GmbH. It is used for qualitative experimental research into character of bulk solid motion in the trough. It is also used to measure the mass productivity depending on fill ratio, sort of bulk solid, angle of inclination and rotational speed of SSC.

It has the following parameters:

$n_{Wn} = 46\ min^{-1}$,	$\eta_{Fn} \approx 0.7$,	$I_{Vn} \approx 1.5\ m^3/h$ ($k_F \approx 0.8$)	
$d_T = 120\ mm$,	$L_T = 2250\ mm$,	$L_W = 2000\ mm$,	$\delta = 0° \dots 60°$
$d_{Wa} = 110\ mm$,	$d_{Wi} = 34\ mm$,	$s_W = 4\ mm$,	$l_{St} = 75\ mm$
Drive:	$P_n = 1.5\ kW$,	$M_n = 126\ Nm$,	$n_W = 2 \dots 188\ min^{-1}$

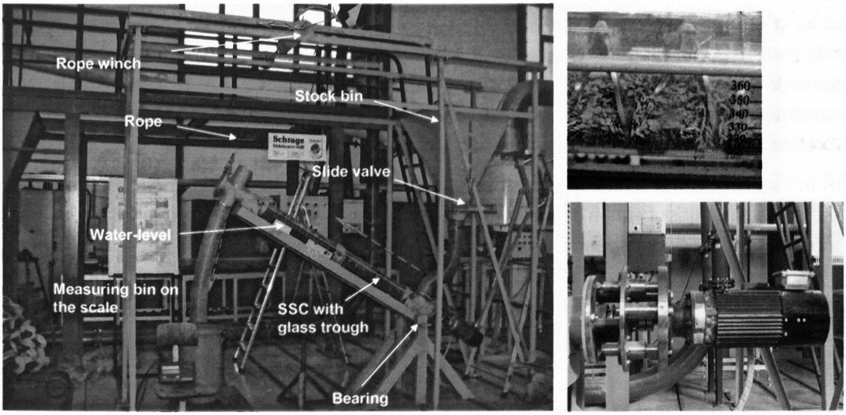

Fig. 6: The test rig and its components (the measuring lines on the glass trough during the transportation of oat and the drive unit)

Bearings are mounted between the trough and supports, so that the inclination of the trough can be varied widely. The trough is made of glass, which allows observation of the run-character and control of the fill ratio. The slide valve of the stock bin and the measuring lines on the glass trough help to install the fill ratio visually. The conveyor drive is supplied with a frequency regulator so that the rotational speed of the screw can be varied. The measuring bin is placed on the scale and a stopwatch is used to measure mass productivity.

The model test rig may be also used to test the troughs and screws with different geometry and material parameters by wide variation of the angle of elevation, drive speed and fill ratio.

5 Criteria for choice of bulk solids and test planning

Following criteria were used for selection of bulk solids:

- Particle size and form
- Bulk density
- Flow properties

For the test series four different bulk solids namely mix granulate (MG - granulate of plastic and rubber), fine-grained sand (Sand), oat and basalt powder (BP) were chosen. They represent three groups of materials with different properties: sand and mix granulate (free flowing, coarse grained, non-compressible and non-cohesive bulk solids), basalt powder (cohesive, badly flowing, powdery with strong fluidization properties bulk solids) and oat (compressible with non-uniform grain form).

All tests were divided into qualitative und quantitative tests in load and no-load operation mode.

In the tests with a HSSC of pilot plant in no-load operating mode the torque was measured with the torsion test shaft at differing rotational speeds n_W = 4; 8; 12; 16; 20 min^{-1} and with a coating of remaining bulk solids in the trough. In the load operating mode, the following values were measured: axial and press loading, total torque and mass throughput I_m for the same bulk solids and rotational speeds n_W and fill ratios $\eta_F \approx$ 0.1...0.2; 0.5; 0.7; 0.9. At the same time the character of bulk solid motion in the HSSC and VSSC was observed. The rotational speed and the fill ratio in VSSC was approx. constant: $\eta_F \approx 1.0$ and n_W = 27 min^{-1}.

In the tests with the model shaftless screw conveyor of the test rig with chosen bulk solids, the mass throughput was measured and the bulk solid motion in the trough was observed at the different rotational speeds n_W = 11; 25; 46 min^{-1}, angles of inclination $\delta \approx$ 0°... 60° (with step: $\Delta\delta \approx$ 3° ... 10°) and fill ratios $\eta_F \approx$ 0.3; 0.7; 0.9 (1.0). Here it was important to determine the inclination fields of a shaftless screw conveyor.

6 Qualitative study of SSCs

Qualitative study deals with analysis of bulk solid motion in the trough of SSC. It helps to understand the physical processes, which happen with the bulk solid in the trough and thereby to develop scientific principles for the design of SSCs correctly.

6.1 Analysis of bulk solid motion in HSSC

In case of HSSCs by small values (η_F < 0.45) of fill ratio the shaftless screw pushes or pulls the bulk solid in the axial direction. The bulk solid moves directly and uniformly as in usual horizontal and lightly inclined screw conveyors (HSCs). Fig. 7 – 10 show, that after the screw starts to rotate, the bulk solid is moved from the static into a dynamic state by offset angle ε (slope angle of surface). When no bulk solid flow motion above the screw flight (known as throw-back) occurs, the conveyance velocity of bulk solid is equal to the axial velocity of the screw $v_F \approx v_W = n_W \cdot l_{St}$ (Fig. 7, 8). The slight throw-back in Fig. 7, 8 occurs only in the contact field because of friction bulk solid/screw.

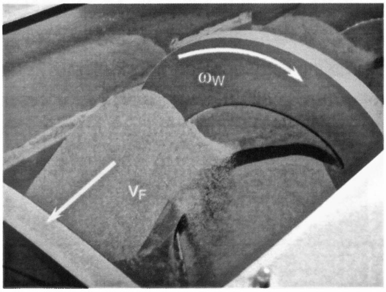

Fig. 7: Sand, $\eta_F \approx 0{,}15$, $n_W = 12\ min^{-1}$
The straightforward uniform motion, $v_F \approx v_W$.

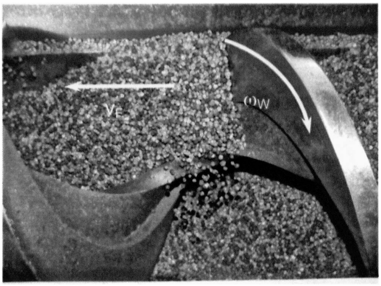

Fig. 8: MG, $\eta_F \approx 0{,}2$, $n_W = 12\ min^{-1}$
The straightforward uniform motion, $v_F \approx v_W$.

The character of bulk solid motion is changed by high values of fill ratio (Fig. 9, 10). The throw-back increases with increasing of fill ratio η_F. Consequently this part of bulk solid has to be conveyed again. Additionally to the straightforward component of bulk solid motion the rotational component occurs. The rotational component increases with the increase of fill ratio. In this case the average conveyance velocity of bulk solid gets smaller as the ideal conveyance velocity $v_F < v_W$ and can only be determined experimentally. The conveyance efficiency increases also with the width of screw (number of screw helical flights). The beginning of the throw-back depends on the properties of the bulk solid as well.

Fig. 10 shows the surface bulk solid motion above the screw flight and the offset angle ε for the oat. Additionally, a strong overlap of the straightforward and rotational components in bulk solid motion was noticed.

The qualitative research shows that the straightforward component of bulk solid motion prevails over the rotational component in the HSSC. The rotational component (Fig. 11) increases as the fill ratio η_F increases and depends on the bulk solid /screw (trough) wall friction ratios and on the properties of the bulk solid (cohesion, adhesion and internal friction).

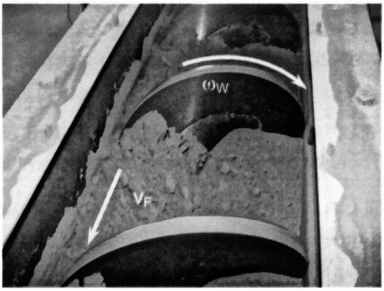

Fig. 9: BP, $\eta_F \approx 0{,}5$, $n_W = 12\ min^{-1}$

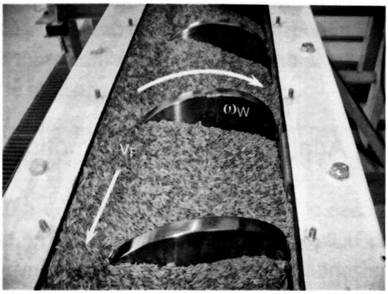

Fig. 10: Oat, $\eta_F \approx 0{,}7$, $n_W = 12\ min^{-1}$

The straightforward component of bulk solid motion prevails over the rotational component. Strong throw-back.

The stronger the cohesive and adhesive properties of bulk solid are and the higher the fill ratio η_F is, the stronger the rotational component in the bulk solid motion is. In contrast, the greater the wall friction coefficient bulk solid/trough μ_{FT} is, and the smaller the wall friction coefficient bulk solids/shaftless screw μ_{FW} is, the smaller rotational component in the bulk solid motion becomes and as a result the HSSC works effectively.

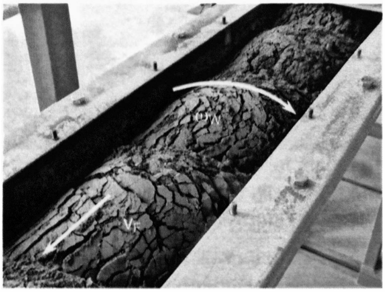

Fig. 11: BP, $\eta_F \approx 0.9$, $n_W = 12\ min^{-1}$

The straightforward component prevails over the rotational component in bulk solid motion

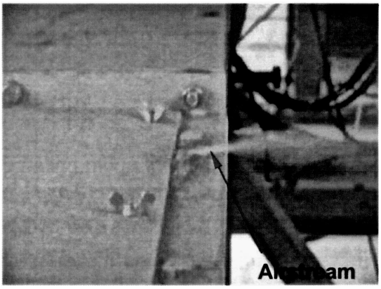

Fig. 12: BP, $\eta_F \approx 1.0$, $n_W = 20\ min^{-1}$

Fluidisation of BP by high rotational speeds of shaftless screw

Figures 9, 11 show the conveyance of basalt powder in HSSC. Even though the straightforward component prevails, the strong rotational component and consequently the throw-back (especially in the contact field screw/bulk solid) were observed. In cohesive bulk solids the internal friction forces are higher than in free flowing bulk solids. Consequently the rotational component in cohesive bulk solids is stronger than in free flowing bulk solids. The conveyance of basalt powder by higher rotational speeds causes its fluidisation (Fig. 12).

The state of the stress condition within bulk solid is very important. By increasing the fill ratio η_F the stress condition in the bulk solid is changed from active to complex (active + passive).

It causes the increase of internal friction in the bulk solid and as a result, an increase of rotational component.

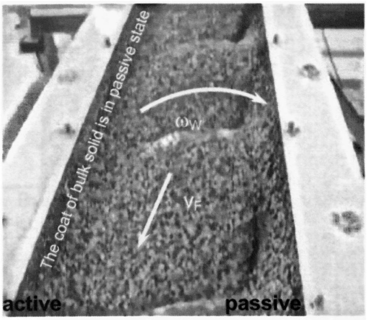

Fig. 13: MG, $\eta_F \approx 1{,}0$, $n_W = 12\ min^{-1}$.

Active und passive zones of stress condition in the bulk solid.

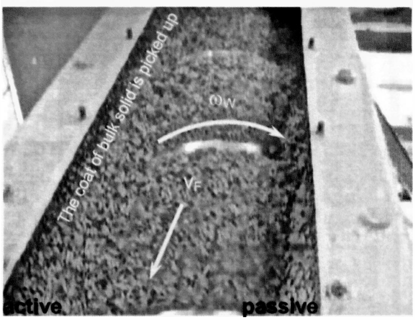

Fig. 14: Oat, $\eta_F \approx 1{,}0$, $n_W = 12\ min^{-1}$

Active und passive zones of stress condition in the bulk solid.

Fig. 13 and 14 show the difference in the stress condition in the bulk solid by conveyance of the mix granulate (l.) and the oat (r.). On the side, where the bulk solid is lifted by the screw from the trough the active stress condition prevails and the friction force screw/bulk solid decreases. In the opposite side, where bulk solid is compressed, the passive stress condition prevails and the friction force bulk solid/screw increases. In this case the complex (active + passive) stress condition is reached.

6.2 Analysis of bulk solid motion in VSSC

In the *vertical SSC* both straightforward and rotational components (Fig. 15) were observed. Here the rotational component of bulk solid motion prevails over straightforward. It is essential to note that the conveyance of bulk solid in the VSSC is possible only by continual feeding with the bulk solid (from HSSC in this study) and that the trough stays almost completely full (the emptying of VSSCs by itself is not possible), so that the fill ratio achieves the value of approx. $\eta_F \approx 1.0$.

The column of bulk solids in the trough of the VSSC rotates with the rotational speed slower than the rotational speed of the shaftless screw, because of wall friction between the bulk solid and the trough. It causes the upward straightforward relative motion of bulk solid, so that the bulk solid motion in the trough has a similar character to a “screw and nut”-motion, like in usual VSCs. Apparently, the conveyance is possible only if the wall friction trough/bulk solid is higher than the wall friction screw/bulk solid. Consequently, the greater the wall friction coefficient bulk solid/trough μ_{FT} is and the smaller the wall friction coefficient bulk solids / screw μ_{FW} is, the more effective conveyance is.

Fig. 15: MG, n_W = 27 min^{-1}.
The filling of the trough by building up a bulk solid column as a result of permanent feeding from HSSC

6.3 Fields of angle of elevation of SSCs

The pilot plant does not allow an investigation of the influence of the angle of elevation on bulk solid motion in the trough and on volumetric throughput.

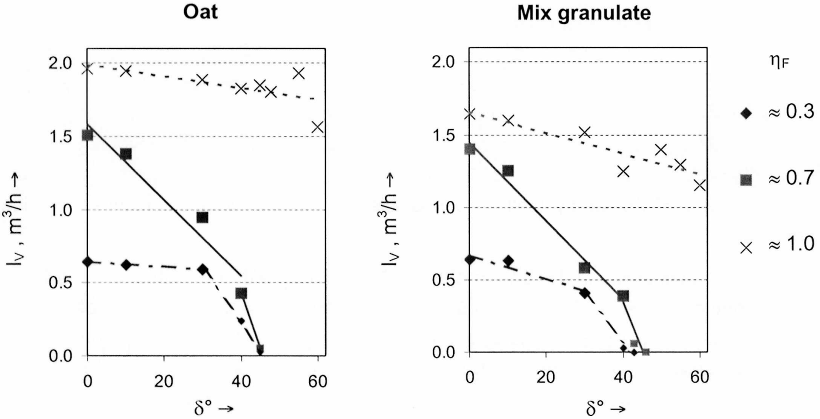

Fig. 16: Volumetric throughput I_V depending on the fill ratio η_F and angle of elevation δ by constant rotational speed n_W = 46 min^{-1} in the test rig for oat (l.) and MG (r.).

The model test rig is used for this purpose. Fig. 16 illustrates the influence of the angle of elevation on the volumetric throughput.

The analysis of Fig. 16 shows that up to a certain angle of elevation, conveyance is possible only after increasing the fill ratio. If the continual feeding from stock bin is stopped, the fill ratio decreases to a certain level and the shaftless screw rotates without emptying the remaining bulk solid from conveyor. Tab. 1 shows the values of angle of elevation and fill ratio for the chosen powder and grained bulk solids, when the throughput of conveyor gets $I_V = 0$.

Tab. 1: Remaining bulk solid depending on fill ratio and angle of elevation (transitional field)

Bulk solid	Rotational speed of screw n_W, min^{-1}	Remaining fill ratio η_{FR}	Angle of elevation $\delta°$	Throughput I_v, kg/s
Basalt powder	11	≈0,3	32	0
		≈0,6	36	
		≈0,9	40	
Oat	11	≈0,3	40	0
		≈0,6	43	
		≈0,9	46	

The experimental results (incl. Tab 1) obtained by the test rig help to define 3 inclination fields of a shaftless screw conveyor (Fig. 17):

The sub-transitional field δ_{STF}°(STF-filed)

In the sub-transitional elevation field conveyance takes place continually and the conveyor can be emptied always completely by itself ($\eta_{FR} = 0$). This elevation field is typical for HSSCs. The general conveyor processes are identical with in the chapter 6.1 in detail documented. The critical angle for this field depends on the bulk solid properties. Tab. 1 shows that by $\delta_{cr} \approx 32°$ the remaining fill ratio is already $\eta_{FR} \approx 0.3$. So that the STF is located in an interval $0° \leq \delta_{STF} < 32°$.

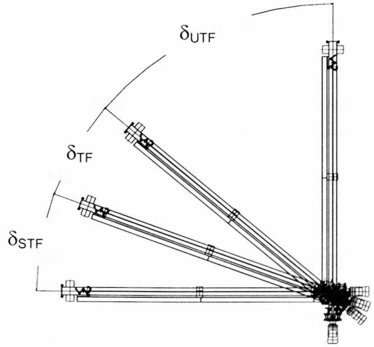

Fig. 17: Three inclination fields of SSC

The upper-transitional field δ_{UTF}° (UTF-filed)

The upper-transitional elevation field is typical for VSSCs. The established conveyor processes here are identical with those described in the chapter 6.2. The SSC does not empty itself in the UTF at all. Remaining fill ratio is always constant $\eta_{FR} \approx 1,0$. Complete emptying of conveyor is possible only if one reduces the angle of elevation to get the STF or one increases the rotational speed substantially (in this case the centrifugal force allows the emptying). Based on the data from Tab. 1 the lowest critical angle is $\delta_{cr} \approx 46°$. Therefore the UTF-field is located in an interval $46° < \delta_{UTF} \leq 90°$.

The transitional field δ_{TF}°(TF-field)

The elevation field in an interval $32° \leq \delta_{TF} \leq 46°$ is emphasized as the transitional field (TF-field). The value of remaining fill ratio depends on bulk solid properties, angle of elevation, rotational speed and was always $0 < \eta_{FR} < 1$. Strong back flow of bulk solid through the internal hole of the screw was observed (Fig 18, 19). Because of this it was complicated to describe the bulk solid motion character. At high rotational speeds, the bulk solid was non-uniformly distributed in the trough. The disadvantage of TF-field is the high values of remaining fill ratio and as a result the low values of throughput. Consequently the conveyance in this field is reasonable only by fill ratio $\eta_F \approx 1,0$. In this case the TF-field has the same characteristics as UTF-field.

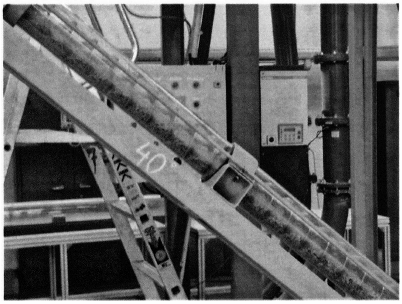

Fig. 18: Oat, TF-field, $\delta = 40°$, $\eta_{FR} \approx 0,3$, $n_W = 11\ min^{-1}$

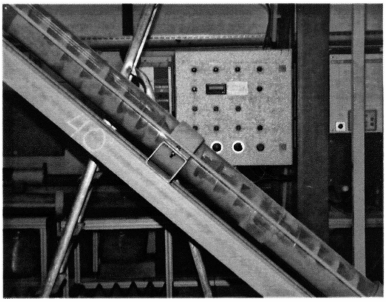

Fig. 19: BP, TF-field, $\delta = 40°$, $\eta_{FR} \approx 0,8 \ldots 0,9$, $n_W = 11\ min^{-1}$

To sum up, it is to be concluded that, there are two elevation fields, which have to be investigated:

- *STF-field*: $0° \leq \delta_{STF} < 32°$,
- *UTF-field* (includes the TF-field): $32° \leq \delta_{UTF} \leq 90°$.

However, here it should be pointed out that the experiments in the model test rig were realized with a glass trough. Hence the results are only partly transferable to the real SSCs. In the case of a glass trough, the conveying process is less efficient than in the real SSC with the steel trough because the wall friction coefficient bulk solid/glass is lesser than bulk solid/steel (with the exception of fine-grained sand). About the relationship between ratios of wall friction coefficients on the one hand and the efficiency of the SSC, on the other hand, was already reported in chapters 6.1 and 6.2.

Therefore the conveyance is more efficient in the real SSCs. It means that the STF-field is wider as well. This is confirmed by the practical experience of the company SPIRAC. Company SPIRAC also gives two intervals for the elevation fields of the SSCs which differ approx. 5 ° from the results in this study:

- *STF-field (SPIRAC)*: $0° \leq \delta_{STF} \leq 35°$,
- *UTF-field* (SPIRAC): $35° < \delta_{UTF} \leq 90°$.

Additionally, it confirms that the results of the qualitative investigations in the test rig are significant.

7 Determination of grain destruction in the HSSCs

For customers from e.g. the food- or agriculture industry, it is important to know how much grain material is destroyed by conveyance with SSC. The grain destruction occurs because of radial clearance, which is a result of tolerances of mechanical components and installation (first of all of the trough and screw). It is clear that the grain destruction is influenced by the value of radial clearance, grain class of the bulk solid and especially by blade thickness s_W.

For this reason the oat in the pilot plat at $n_W = 16\ min^{-1}$ and $\eta_F \approx 0{,}2$ was conveyed. The fill ratio $\eta_F \approx 0{,}2$ allows comparison with the grain destruction in horizontal SSC and SC. The test sample before and after conveyance was analyzed. For determination of grain destruction the sieve analysis was used. Fig. 20 illustrates the results of sieve analysis for the oat probe before and after conveyance. The sieve analysis shows, that during conveyance with $\eta_F \approx 0{,}2$ approximately $m_{Dtot} \approx 15$ % of the oat in the pilot plant were destroyed.

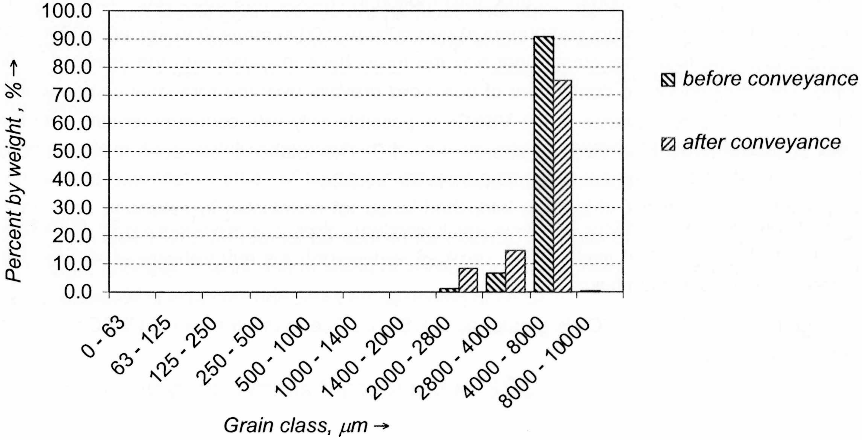

Fig 20: The results of sieve analysis for the oat probe before and after conveyance. (total grain destruction in pilot plant is approx. 15%).

The grain destruction could occur only in horizontal and inclined SSCs of pilot plant, because the value of radial clearance in vertical SSC is higher than the max. grain size of oat. Because of this, it is supposed that VSSC of pilot plant does not influence the total result of grain destruction. The horizontal and inclined SSCs of pilot plant have similar characteristics, so it could be supposed that in each of the conveyors only half of the total grain destruction occurs $m_{DHWF} \approx m_{DGWF} \approx 7{,}5$ %. This assumption should be discussed.

The experimental results for the oat in [6], [19] show, that the total grain destruction in the *high-performance screw conveyor pilot plant* is approx. $m_{Dttot} \approx 23$ % and the geometry parameters are very similar to those described in this study. This could be explained by the markedly higher rotational speeds of the screw in SCs compared to SSCs, which result the higher forces. The results of the total grain destruction in both pilot plants could be compared provisionally only, because the influence of the rotational speed, radial clearance and blade thickness on the grain destruction has not been completely investigated.

Although the total grain destruction in HSSCs cannot be decreased, the mass throughput could be increased by increasing the fill ratio. This result shows that conveyance in HSSCs is reasonable only at high fill ratios.

8 Concluding remarks

The use of SSCs instead of SCs makes sense only in special application cases because of low throughput values.

Due to considerable differences between HSCs and HSSCs the principles of calculation for HSCs cannot be applied for HSSCs.

The qualitative study shows that the operating characteristics of HSSCs and bulk solid properties influence the motion character of bulk solid in the trough significantly. By low fill ratios only straightforward component of bulk solid motion in HSSCs was observed. Increasing the fill ratio causes the rotational component in bulk solid motion in addition to the straightforward component. The rotational component and the throw-back increase with the increase of fill ratio. The straightforward component of bulk solid prevails over the rotational component in the HSSCs. The conveyance in the VSSCs is possible only with continual feeding with the bulk solid and by fill ratio value of approx. $\eta_F \approx 1.0$. The rotational component of bulk solid prevails over the straightforward component in the VSSCs.

The qualitative study helped to define the inclination fields of a shaftless screw conveyor. There are two inclination fields, which have be considered: the sub-transitional and the upper-transitional elevation fields.

The grain destruction in HSCs is greater as in HSSCs. Due to this the use of HSSCs for careful conveyance is preferable.

Theoretical and experimental study of horizontal and lightly inclined shaftless screw conveyors

Part 1: Theoretical study of horizontal and lightly inclined shaftless screw conveyors

Abstract

This paper consists of two parts and is concerned with horizontal and lightly inclined shaftless screw conveyors (HSSCs). It describes some of the necessary knowledge for the designing and use of HSSCs. The first part focuses on theoretical study of HSSCs. The second part deals with their quantitative study. The purpose of this work is to develop scientific principles for the calculation and design of HSSCs and to define the limits of their application.

1 Introduction

The shaftless screw conveyors open up a new and special areas of application for screw conveyance, which are determined according to special properties of the bulk solids. The SSC expands the screw conveyor's field of application and is used for those bulk solids, when the usual screw conveyor cannot be used. The SSC can be used in the transport of cohesive, adhesive, semisolid, paste, fibered bulk solids and solid-water mixtures. SSCs are mainly used in sewer, dust, tree, pulp, paper, food processing, agriculture and building industry plants.

The results of the qualitative research in SSCs were already reported (see above). The theoretical and quantitative study of SSCs for different bulk solids was not conducted till the last time. The principles of calculation for usual horizontal and lightly inclined screw conveyors (HSCs) in DIN 15262 [4] cannot be applied for HSSCs, because of considerable differences in design, principle of work and in areas of application (see above). The reason for this study is the absence of scientific principles for designing of HSSCs.

2 Volumetric- and mass throughput in SSCs

2.1 Effective diameter of trough and volume of shaftless screw

It is not possible to describe analytically the processes in radial clearance of SSC. Analysis of bulk solid motion in the trough shows that the part of bulk solid in the clearance is picked up due to internal friction within the bulk solid. In view of this, for the calculating of SSCs the effective diameter is introduced, which includes the thickness s_{Schl} of wear-resistant liner.

The effective diameter of the SSC with low angle of elevation (HSSCs), which have the U-shaped troughs is calculated as:

$$d_T = (d_{TU} - 2 \cdot s_{Schl}) > d_{Wa} . \quad (1)$$

The O-shaped troughs are typical for VSCs and VSSCs with high angle of elevation. For the same screw diameters in a catalogue they have the trough's diameters, which are smaller as by HSSCs to reduce the radial clearance.

The conveyance in HSSCs is realized with high values of fill ratio 0.5 $\leq \eta_F \leq$0.9 comparing with HSCs. The fill ratio in VSSCs is always $\eta_{Fv} \approx$1.0. The value of shaftless screw has to be taken into account.

The calculation of trough volume using effective diameter and length:

$$V_T = \frac{d_T^2 \cdot \pi}{4} \cdot L_T . \quad (2)$$

The maximum volume V_{Fmax}, which could be occupied by the bulk solid in the trough is the difference between the trough V_T and screw volumes V_W:

$$V_{F\max} = V_T - V_W = \frac{\pi}{4} \cdot d_T{}^2 \cdot L_W - V_W = V_T \cdot \eta_V , \quad (3)$$

The volumetric ratio η_V shows how much usable volume of a trough is occupied by the volume of the shaftless screw and can be calculated as the ratio between the screw and the trough volume according to Eq. (3):

$$\eta_V = \frac{V_T - V_W}{V_T} = 1 - \frac{V_W}{V_T} . \quad (4)$$

The volume of one shaftless screw coil is calculated as:

$$V_{Ww} = \frac{s_W}{cos\,\alpha_a} \cdot \left[\frac{(l_{St})^2}{4\pi} ln \frac{\sqrt{(2 \cdot \pi \cdot r_{Wa})^2 + (l_{St})^2} + 2\pi r_{Wa}}{\sqrt{(2 \cdot \pi \cdot r_{Wi})^2 + (l_{St})^2} + 2\pi r_{Wi}} + \frac{r_{Wa}}{2} \sqrt{(2 \cdot \pi \cdot r_{Wa})^2 + (l_{St})^2} - \frac{r_{Wi}}{2} \sqrt{(2 \cdot \pi \cdot r_{Wi})^2 + (l_{St})^2} \right] \quad (5)$$

If in Eq. (5) the pitch l_{St} = *0*, than helix angle of the screw flight corresponding to the outer diameter α_a = *0 (cos*α_a *= 1)*, the Eq. (5) takes the form of:

$$V_{Ring} = s_W \cdot \pi \cdot (r_{Wa}^2 - r_{Wi}^2) . \quad (6)$$

The Eq. (6) represents the volume of the ring. The volume of one shaftless screw coil is greater than the volume of ring (by the same geometry parameters): $\boldsymbol{V_{Ww} > V_{Ring}}$

The volume of the shaftless screw is the product of the volume of one shaftless screw coil V_{Ww} and the number of pitches z_W:

$$V_W = z_W \cdot V_{Ww} . \quad (7)$$

The number of pitches of the shaftless screw is: $z_W = \frac{L_W}{l_{St}}$. (8)

If the shaftless screw consists of many helical flights and its total volume has to be calculated, then the volume of each helical flight should be calculated separately and summed.

It is to be noticed that the Eq. (5) delivers useful results only for the industrial-made shaftless screws with usual thickness and diameter of screw blade.

2.2 Geometry of shaftless screw and conveyance velocity

The basic principles of calculation for SSCs were developed based on DIN 15262 [4], which describes the design oh HSCs. In spite of this fact, there are a lot of different features, what are important and discussed below.

The pitch l_{St} of the screw is selected depending on the bulk solid properties and the angle of elevation:

$l_{St} = (0,6...1,1) \cdot d_{Wa}$,

Based on practical experience, the minor values of the pitch are considered for difficult-to-transport bulk solids and steeper angles of elevation.

The screw width b_W is very important for the motion of the bulk solids. Transportation of non-cohesive and homogeneous bulk solids by higher angles of elevation requires wide screws. Such shaftless screws can be welded from two or three helical flights.

The pitch l_{St} should be chosen smaller by growing outside diameter d_{Wa}.

All shaftless screws may be divided into 3 groups. For this purpose the coefficient of radii ratio k_r is introduced.

$$k_r = \frac{b_W}{r_{Wa}} = \frac{r_{Wa} - r_{Wi}}{r_{Wa}} < 1.$$

The coefficient of radii ratio k_r shows, to what extent the width of screw blade covers the cross section of the shaftless screw.

Following coefficients of radii ratio are used in the practice (based on catalogue data of DIM GmbH and Wildfellner GmbH):

One helical flight: $k_{rI} \approx 0,27 ... 0,76$,

Two helical flights: $k_{rII} \approx 0,46 ... 0,88$,

Three helical flights: $k_{rIII} \approx 0,83 ... 0,97$.

The conveyance velocity v_F in HSSCs is calculated as:

$$v_F = v_W \cdot k_F \cdot k_\delta \qquad (9)$$

The axial velocity of the screw v_W is calculated according to [4]:

$$v_W = n_W \cdot l_{St}. \qquad (10)$$

The velocity coefficient k_F expresses to which degree the conveyance velocity v_{F0} of bulk solid by the angle of elevation $\delta = 0°$differs from the axial velocity of the screw v_W:

$$k_F = \frac{v_{F0}}{v_W} = \frac{I_{m\exp 0}}{I_{mth}}. \tag{11}$$

The velocity coefficient k_F depends on bulk solid properties, conveyor and operating characteristics (rotational speed, fill ratio and geometry of shaftless screw).

The velocity coefficient k_δ expresses to which degree the conveying velocity $v_{F\delta}$ of bulk solid at the angle of elevation $\delta \neq 0°$ differs from the conveyance velocity v_{F0} of bulk solid at the angle of elevation $\delta = 0°$.

$$k_\delta = \frac{v_{F\delta}}{v_{F0}} = \frac{I_{m\exp\delta}}{I_{m\exp 0}}, \tag{12}$$

where I_{mexp0} , $I_{mexp\delta}$ are the measured values of throughput by the angles of elevation 0° and δ°. If the angle of elevation is $\delta = 0°$, then $k_\delta = 1{,}0$.

The velocity coefficient $k_{F\delta}$ is the product of the velocity coefficients k_F and k_δ and expresses to which degree the conveyance velocity $v_F = v_{F\delta}$ of bulk solid at the angle of elevation $\delta \neq 0°$ differs from the axial velocity of the screw v_W:

$$k_{F\delta} = k_F \cdot k_\delta = \frac{v_F}{v_W} = \frac{v_F}{n_W \cdot l_{St}} = \frac{I_{m\exp\delta}}{I_{mth}}. \tag{13}$$

All the velocity coefficients have to be determined experimentally.

For VSSCs with high angles of elevation and $\eta_F \approx 1{,}0$ only the velocity coefficient $k_{F\delta}$ is considered.

2.3 The fill ratio in SSCs

The fill ratio η_F is calculated as:

$$\eta_F = \frac{A_F}{\eta_V \cdot A_T} = \frac{F_{F\exp}}{F_{F100}}, \tag{14}$$

where F_{Fexp} is the actual weight of the bulk material in the trough of SSC.

The maximum weight of the bulk material in the trough of SSC can be calculated from:

$$F_{F100} = V_{F\max} \cdot \rho_b \cdot g = \eta_V \cdot V_T \cdot \rho_b \cdot g. \tag{15}$$

The bulk solid volume in the trough of SSC is the result from the difference between the trough and screw volume. It may be calculated in consideration of the fill ratio η_F as follows:

$$V_F = (V_T - V_W) \cdot \eta_F = \eta_V \cdot V_T \cdot \eta_F, \tag{16}$$

With Eq. (16) the mass of bulk solid can be calculated as:

$$m_F = \rho_b \cdot V_F = \rho_b \cdot \eta_V \cdot V_T \cdot \eta_F,$$

2.4 The volumetric- and mass throughput

The volumetric and mass throughput of a conveyor are given by:

$$I_V = A_F \cdot v_F , \tag{17}$$

$$I_m = I_V \cdot \rho_b , \tag{18}$$

where A_F is the conveyance cross sectional area and v_F is the conveyance velocity.

In accordance with DIN 15262 [4], the conveyance cross sectional area for SSCs is defined as:

$$A_F = \eta_F \cdot A_T = \eta_F \cdot d_T^2 \cdot \frac{\pi}{4} . \tag{19}$$

Note that the fill ratio η_F of HSSCs is considerably greater than of common HSCs.

The volumetric throughput of HSSCs results from following equation:

$$I_V = d_T^{\ 2} \cdot \frac{\pi}{4} \cdot n_W \cdot l_{St} \cdot \eta_F \cdot \eta_V \cdot k_F \cdot k_\delta \tag{20}$$

The volumetric throughput of VSSCs ($\eta_F \approx 1{,}0$) is the result of:

$$I_V = d_T^{\ 2} \cdot \frac{\pi}{4} \cdot n_W \cdot l_{St} \cdot \eta_V \cdot k_{F\delta} \tag{21}$$

3 Calculation of mechanical characteristics for HSSCs

The main mechanical characteristics include, among others, the torque M_F and the axial force F_{ax} due to motion resistance resulting fictive coefficients of motion resistance λ_0, λ_F, as well as the specific power P_{spc}. They refer to the mechanical characteristics of conveyor.

The following points are assumed to develop the principles of calculation of mechanical characteristics for HSSCs:

- The steady-state of conveyance in the HSSCs. The fill ratio is constant in each point of the trough.
- The bulk solid properties, which are determined in the Bulk Solid Lab of IFSL did not change during conveyance.
- The bulk solid is moved in the axial direction only. This assumption allows for the application of the “screw and nut”-motion model to HSSCs in consideration of velocity coefficients.
- The influences of radial clearance, tolerances of mechanical components and installation are not considered.

3.1 Simplified calculation of mechanical characteristics for HSSCs

The simplified principles of calculation for HSSCs are developed primarily for industries to help them determine the total torque, axial force and power for HSSCs.

The DIN 15262 [4] was developed to design and calculate the usual HSCs with angles of elevation δ $\leq 20°$ and fill ratio values $\eta_F \leq (0,15 \ldots 0,45)$. The calculation principles in DIN 15262 [4] may be approximately applied for calculation of HSSCs in consideration of shaftless screw weight, when the fill ratio value is interval of $0 < \eta_F < 0,3$ (0,45), i.e. when throwback is very small or non-existent. In this case, the characteristics of bulk solid motion in HSCs and HSSCs are similar. The problem is that HSSCs work efficiently only with high fill ratios ($\eta_F > 0,5$) and consequently, the DIN 15262 [4] cannot be applied.

- *The total conveyor power P_W of HSSCs is:*

$$P_W = P_0 + P_{St} + P_F = g \cdot L_W \cdot \cos\delta \cdot \left[\lambda_0 \cdot \overline{m}_W \cdot v_u + I_m(\lambda_F + \tan\delta)\right], \tag{22}$$

where the screw velocity due to its rotation results from the well known equation:

$$v_u = 2 \cdot \pi \cdot n_W \cdot r_{Wa} \tag{23}$$

In horizontal SSC (HSSC) is $\cos\delta = 1$, $\tan\delta = 0$ and consequently $P_{St} = 0$.

According to this the Eq. (22) the total conveyor power of HSSC is calculated as:

$$P_W = P_0 + P_F = g \cdot L_W \cdot \left[\lambda_0 \cdot \overline{m}_W \cdot v_u + I_m \cdot \lambda_F\right], \tag{24}$$

On the other hand the total power may be determined from:

$$P_W = P_0 + P_F = M_W \cdot \omega_W = (M_{W0} + M_F) \cdot 2 \cdot \pi \cdot n_W \tag{25}$$

The generalization of the experimental results for all SSCs is problematic, because the measured values (M_{W0}, M_W, F_{ax}, I_m or P_0 and P_W) are obtained for defined SSCs with specific operating characteristics (geometry of conveyor units, fill ratio, rotational speeds). To avoid this problem, the velocity coefficients k_F , k_δ, the specific power P_{spc} and the fictive coefficients of motion resistance λ_0 in no-load and λ_F in load operation mode were introduced.

The fictive coefficients of motion resistance were introduced, because some of motion resistances cannot be estimated theoretically.

- *The fictive coefficient of motion resistance λ_0 in no-load operation mode in HSSC is:*

$$\lambda_0 = M_{W0} \cdot \frac{2 \cdot \pi \cdot n_W}{m_W \cdot g \cdot v_u} = \frac{M_{W0}}{m_W \cdot g \cdot r_{Wa}} \tag{26}$$

- *The fictive coefficient of motion resistance λ_F in load operation mode in HSSC is given by:*

$$\lambda_F = M_F \cdot \frac{2 \cdot \pi \cdot n_W}{m_F \cdot v_F \cdot g} = (M_W - M_{W0}) \cdot \frac{2 \cdot \pi \cdot n_W}{I_m \cdot g \cdot L_W} \tag{27}$$

The specific power P_{spc} is important for comparison and analysis of the experimental results measured by different SSCs. The specific power P_{spc} is the quotient of power consumption P_F of SSC, which is required to achieve the desired mass throughput I_m, and this mass throughput I_m; whereas the result is scaled on 1 m:

$$P_{spc} = \frac{P_F}{I_m \cdot L_W} = \frac{2 \cdot \pi \cdot n_W}{L_W} \cdot \frac{M_F}{I_m}, \tag{28}$$

or:

$$P_{spc} = \frac{P_W - P_0}{I_m \cdot L_W} = \frac{2 \cdot \pi \cdot n_W}{L_W} \cdot \frac{(M_W - M_{W0})}{I_m}. \tag{29}$$

where the M_{W0}, M_W und I_m are measured in experiment values.

The fictive coefficient of motion resistance λ_S for the usual HSCs is available for different bulk solids in DIN 15262 [4]. The λ_0, λ_F, P_{spc}, k_F, k_δ -values of the SSC should be investigated for the different bulk solids, angles of elevation and rotational speeds of conveyor.

For strength calculation of a conveyor units the equations for total torque and axial force are required. They can be derived from Eq. (24) – (27) in consideration of known λ_0, λ_F, k_F, k_δ - values, which are general for all SSCs. The total torque M_W is:

$$M_W = \frac{(\lambda_0 \cdot \overline{m}_W \cdot v_u + \lambda_F \cdot I_m) \cdot L_W \cdot g}{\omega_W}. \tag{30}$$

In [7], [21], [24] the equation for calculating the axial force of the drive screw F_{Sax} is used to estimate the axial force on the screw of usual screw conveyor. This equation gives the relation between turning torque and the axial force developed between a screw and nut. It is assumed that the axial force acts at the mean pitch diameter. In reality the position of the point of application of the axial force depends on conveyor's parameters as well as on bulk solid. This is why this equation should be extended for SSCs by a correction factor k_{ax}:

$$F_{Sax} = k_{ax} \cdot \frac{2 \cdot M_W}{d_{Wm} \cdot \tan(\alpha_m + \varphi_{FW})}. \tag{31}$$

The correction factor k_{ax} or the adaptation of the Eq. (31) to the reality is discussed in the 2nd part of this article closer.

3.2 Theoretical model for calculation of mechanical characteristics for HSSCs

In the model, the bulk solid body in the screw chamber is divided into two parts. After this the action of its gravities on the shaftless screw and the trough are considered. With the appropriate decomposition of forces, several friction forces and friction torques can be determined. From the bulk solids masses m_1, and m_2 using auxiliary angles β_1 and β_2 the forces F_{R1} and F_{R2} (friction forces between the shaftless screw and the bulk solid) and F_{ax1} and F_{ax2} (axial forces acting from the shaftless screw to the bulk solid) may be determined. Then it is possible to calculate the total torque, axial force acting to the shaftless screw and conveyor power. Fig. 1 and 2 show the sketch of forces and torques acting from the shaftless screw to the bulk solids.

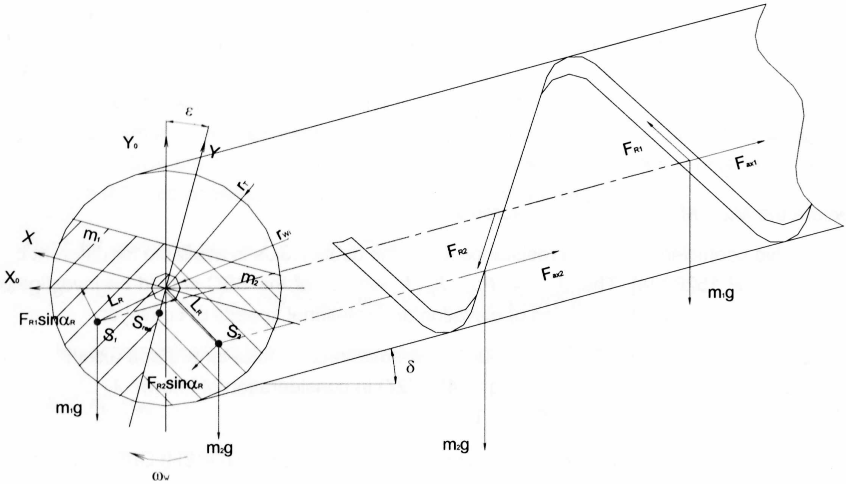

Fig 1: Forces and torques acting on the bulk solids body in a screw chamber at a steady-state condition in HSSCs.

The axial forces acting from the shaftless screw to the bulk solids are given by:

$$F_{ax1} = m_1 \cdot g \cdot \sin\delta + (m_1 \cdot g \cdot \cos\delta - F_{R1} \cdot \sin\alpha_R \cdot \cos\beta_1) \cdot \mu_{FT}, \tag{32}$$

$$F_{ax2} = m_2 \cdot g \cdot \sin\delta + (m_2 \cdot g \cdot \cos\delta + F_{R2} \cdot \sin\alpha_R \cdot \cos\beta_2) \cdot \mu_{FT}. \tag{33}$$

The frictional forces in the screw chamber because of friction between the mass parts m_1, m_2 and the shaftless screw are:

$$F_{R1} = F_{ax1} \cdot \sin\alpha_R \cdot \mu_{FW}, \tag{34}$$

$$F_{R2} = F_{ax2} \cdot \sin\alpha_R \cdot \mu_{FW}. \tag{35}$$

The Eq. (32) – (35) help to determine the frictional forces F_{R1} und F_{R2}:

$$F_{R1} = \frac{m_1 \cdot g \cdot \sin\alpha_R \cdot \mu_{FW} \cdot (\sin\delta + \cos\delta \cdot \mu_{FT})}{1 + \mu_{FT}\mu_{FW} \cdot \sin^2\alpha_R \cdot \cos\beta_1}, \tag{36}$$

$$F_{R2} = \frac{m_2 \cdot g \cdot \sin\alpha_R \cdot \mu_{FW} \cdot (\sin\delta + \cos\delta \cdot \mu_{FT})}{1 - \mu_{FT}\mu_{FW} \cdot \sin^2\alpha_R \cdot \cos\beta_2}. \tag{37}$$

At a steady-state condition, all torques due to the bulk solid motion relative to the screw axis can be expressed by the following equation:

$$(m_1 + m_2) \cdot g \cdot |y_{res0}| \cdot \sin\varepsilon = (F_{R1} + F_{R2}) \cdot L_R \cdot \sin\alpha_R. \tag{38}$$

For the masses m_1, m_2 and for the total mass m of bulk solid in the screw chamber the following equation is valid:

$$m = m_1 + m_2 . \tag{39}$$

The lever arm of the frictional forces L_R , the auxiliary angles β_1 and β_2, and resulting ordinates of centre of gravity y_{res0} for cross section of bulk solid body can be determined from coordinates of centres of gravity of the mass parts m_1, m_2.

$$y_{res0}, \alpha_R, L_R = f\{r_T, \eta_F\}. \tag{40a}$$

$$\beta_1, \beta_2 = f\{r_T, \eta_F, \varepsilon\}. \tag{40b}$$

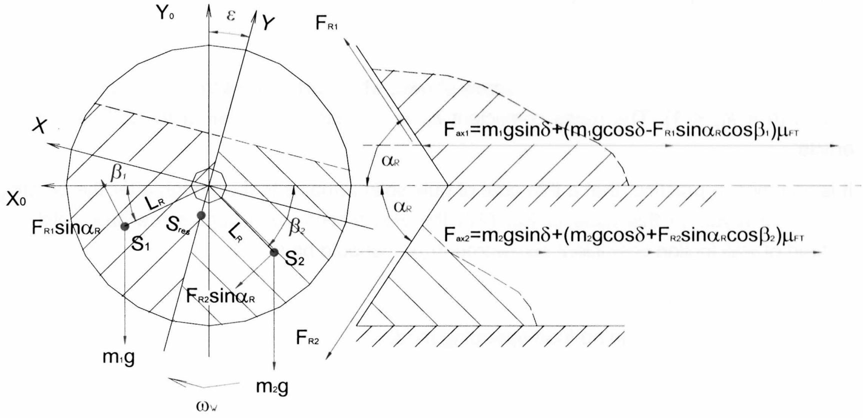

Fig 2: The static balance of torques and forces acting on the bulk solids body in a screw chamber at steady-state condition in HSSCs

The equation system (36) – (40a,b) could be transformed into an equation (41) with only one unknown ε as:

$$\sin\varepsilon = \frac{\sin^2\alpha_R \cdot \mu_{FW} \cdot (\sin\delta + \cos\delta \cdot \mu_{FT}) \cdot L_R}{|y_{res0}|} \times$$

$$\left(\frac{1}{1-\mu_{FT}\mu_{FW} \cdot \sin^2\alpha_R \cdot \cos\beta_2} + \frac{1}{1+\mu_{FT}\mu_{FW} \cdot \sin^2\alpha_R \cdot \cos\beta_1} \right), \tag{41}$$

where: $\sin\varepsilon = f\{r_T, l_{St}, \delta, \mu_{FT}, \mu_{FW}, \eta_F\}$.

The Eq. (41) can be solved only numerically. After then all significant forces, torques and as a result a power consumption of HSSCs can be calculated.

The total axial force acting on the shaftless screw and the power consumption due to this axial force are:

$$F_{ax} = \left(F_{ax1} + F_{ax2}\right) \cdot z_W . \quad (42)$$

$$P_{ax} = F_{ax} \cdot v_F = \left(F_{ax1} + F_{ax2}\right) \cdot z_W \cdot v_F . \quad (43)$$

The total frictional force between the bulk solid and the trough (wear-resistant liner) is:

$$F_{RT} = \left[m \cdot g \cdot cos\,\delta + sin\,\alpha_R \cdot \left(F_{R2} \cdot cos\,\beta_2 - F_{R1} \cdot cos\,\beta_1\right)\right] \cdot \mu_{FT} \cdot z_W . \quad (44)$$

The torque and power consumption due to the friction between the bulk solid and shaftless screw are given by:

$$M_{FW} = z_W \cdot \left(F_{R1} + F_{R2}\right) \cdot L_R \cdot sin\,\alpha_R , \quad (45)$$

$$P_{FW} = \omega_W \cdot z_W \cdot \left(F_{R1} + F_{R2}\right) \cdot L_R \cdot sin\,\alpha_R . \quad (46)$$

The torque due to the friction between the shaftless screw and trough in no-load operating mode may be estimated in considering of mass coefficient k_W as:

$$M_{W0} = k_W \cdot m_W \cdot g \cdot \mu_{WT} \cdot r_{Wa} \cdot cos\,\delta , \quad (47)$$

The mass coefficient k_W of shaftless screw shows, what part of the screw is supported by the trough ($0 < k_W < 1$). The mass coefficient k_W is discussed in detail in the 2nd part of this article.

It is common in practice, that a thin coat of bulk solid remains in the trough after the empting of the conveyor. In this case in Eq. (47) the wall friction coefficient screw/bulk solid μ_{FW} instead of wall friction coefficient screw/trough μ_{WT} should be taken:

$$M_{W0} = k_W \cdot m_W \cdot g \cdot \mu_{FW} \cdot r_{Wa} \cdot cos\,\delta , \quad (48)$$

The power consumption in no-load operating mode is:

$$P_0 = M_{W0} \cdot \omega_W . \quad (49)$$

The total conveyor power and the total torque are given by:

$$P_W = P_{ax} + P_{FW} + P_0 , \quad (50)$$

$$M_W = \frac{P_W}{\omega_W} . \quad (51)$$

The torque due to the friction of bulk solid in conveyor is computed as:

$$M_F = M_W - M_{W0} = \frac{P_F}{\omega_W} . \quad (52)$$

The conveyor power P_W calculated by means of theoretical model does not consider the influence of all motion resistances in load operation mode. Some of them cannot be determined theoretically, because of:

- The complex stress condition in the bulk solid,
- Specific influence of bulk solid properties (fluidisation by powder bulk solids, dependence on cohesion, adhesion, internal friction and consolidation state),
- The influence of operating parameters,

- The short-term blocking of the shaftless screw because of jamming of particles between the screw blade and trough,
- Additional motion resistance in operating start mode.

All of these motion resistances result in the real total conveyor power, which is larger than its theoretical value. Due to this, the theoretical model should be calibrated to real conditions.

The theoretical model allows calculating not only of the total values of torque, axial force and power of conveyor, but also of its parts, which may be used in strength and tribological calculation of conveyor's elements.

Theoretical and experimental study of horizontal and lightly inclined shaftless screw conveyors

Part 2: Quantitative study of horizontal and lightly inclined shaftless screw conveyors

1 Goals of quantitative study of HSSCs

The large-scale pilot plant and model test rig were built with the purpose of qualitative and quantitative study of HSSCs and verification of scientific principles for the calculation and design from Part 1. The equipment and technical dates of both pilot plants are described in the article "Research on shaftless screw conveyors" (see above).

Quantitative study of HSSCs has following goals:

- Determination of volumetric- and mass productivity of HSSCs depending on bulk solid and operating characteristics (fill ratio, rotational speed and angle of elevation). It result velocity coefficients k_F, k_δ.
- Determination of mechanical characteristics (total torque and axial loading on the screw, which result fictive coefficient of motion resistance λ_0, λ_F and specific power of conveyor P_{spz}) depending on bulk solid and operating characteristics.

2 Experimental study of conveyance velocity in HSSCs

Determination of (mass-) volumetric productivity allows calculation of velocity coefficients k_F, k_δ depending on bulk solid and operating characteristics. The velocity coefficients are important for design of HSSCs. They may be determined with equations (11) – (13) from Part 1.

Qualitative study of SSCs [Part 1] shows that motion character of bulk solid in the trough depends not only on bulk solid properties, fill ratio and rotational speed, but also on angle of elevation. Fig. 1 illustrates experimental results for velocity coefficient k_δ. For this reason the mass productivity in the model test rig was measured. The velocity coefficient k_δ decreases with increasing of angle of elevation δ and depends on fill ratio and bulk solid properties. It is important to point out that for fill ratio interval $0 < \eta_F \leq 0{,}9$ and from defined value of angle of elevation the velocity coefficient k_δ decreases dramatically and achieves the value of $k_\delta = 0$. This confirms the existence of inclination fields of SSCs.

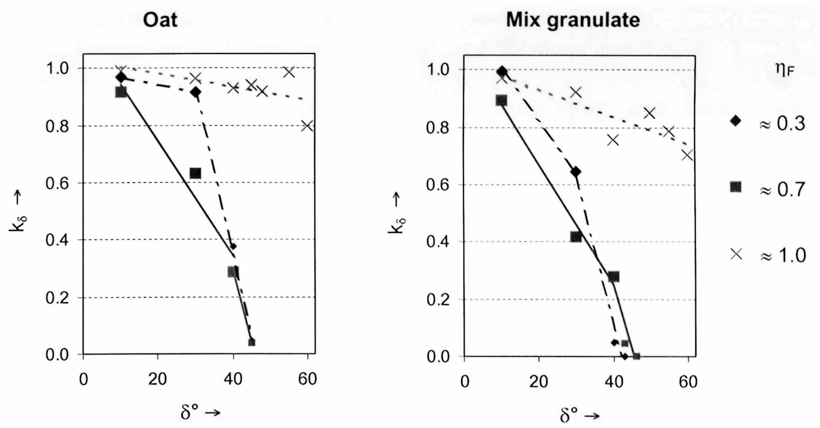

Fig. 1: Velocity coefficient k_δ depending on fill ratio η_F and angle of elevation δ in test rig by conveyance of oat (l.) and mix granulate (r.) with rotational velocity n_W = 46 min^{-1}

From the diagrams in Fig. 1 it follows that from angle of elevation δ > 20° and with high values of fill ratio 0,3 < η_F ≤0,9 the velocity factor k_δ decreases more sharply, than with fill ratio η_F ≤0,3 and also than with η_F ≈1,0. It is already reduced to around half with δ ≈30°. Such behavior of the velocity coefficient k_δ may be explained by:

- strong backflow of bulk solid through the inner diameter of shaftless screw and
- an increase of rotational component in the bulk solid motion by higher angles of elevation δ°.

This behavior of k_δ should be taken into consideration, when the angles of elevation fields in the article "Research on shaftless screw conveyors" (see above) are specified. This consideration is important, because the SSCs are effective only with high values of fill ratio. Hence the sub-transitional elevation field in the article "Research on shaftless screw conveyors" (see above) should be reduced from δ ≈32° to δ ≈20°, especially for grained bulk solids. The other alternative is the use of shaftless screw with three helical fights.

In summary the fields of angle of elevation in the article "Research on shaftless screw conveyors" (see above) can be redefined as follows:

The sub-transitional field (STB-field):	η_F ≤0,3	0° ≤δ_{STB} < 32°,
	0,3 < η_F ≤0,9	0° ≤δ_{STB} < 20°,
The upper-transitional field δ_{UTF}° (UTF-filed):	η_F ≈1,0	(20°) 32° ≤δ_{UTF} ≤90°.

This addition counts of course as a typical shaftless screws, which are used in industry.

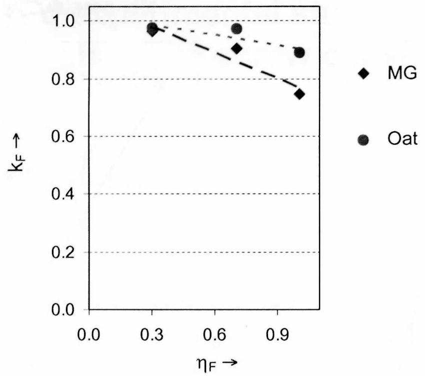

Fig. 2 Velocity coefficient k_F depending on fill ratio for oat and mix granulate by n_W = 46 min^{-1}

The velocity coefficient k_F depends on bulk solid properties and decreases with the increase of the fill ratio, because of the increase of rotational component and of the strong throw-back (it is assumed that the rotational speed in interval of $0 < n_W < 50$ min^{-1} does not influence the velocity coefficient).

The next step in this study is analysis of conveyance velocity depending on rotational speed and fill ratio in HSSC of pilot plant at steady-state condition. Fig. 3 presents the conveyance velocity v_F for basalt powder. The conveyance velocity depends on rotational speed n_W and on fill ratio η_F from its defined value. It decreases with the increase of fill ratio and rises roughly linearly with the increase of rotational speed. Two fields should be distinguished:

Field 1: $\eta_F \leq (0,1...0,2)$, wo $v_F \approx v_W$

and

Field 2: $\eta_F > (0,1...0,2)$, wo $v_F < v_W$.

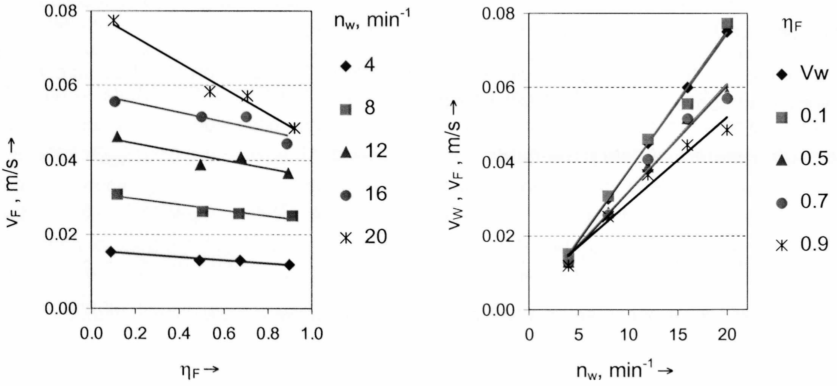

Fig. 3: Conveyance velocity depending on rotational speed n_W and fill ratio η_F for basalt powder

Velocity coefficient k_F (Fig. 4) resulting from conveyance velocity depends on fill ratio η_F and bulk solid properties but barely depends on the usual rotational speed $n_W < 30\ min^{-1}$. When no throw-back occurs, the conveyance velocity is equal to the axial velocity of the screw $v_F \approx v_W$. The velocity coefficient is then $k_F \approx 1$. The critical fill ratio, when throw-back occurs depends on bulk solid properties.

Figure 4 summarises experimental results for velocity coefficient k_F. For the usual rotational speeds the velocity coefficient k_F depends on bulk solid properties and decreases by increasing of fill ratio.

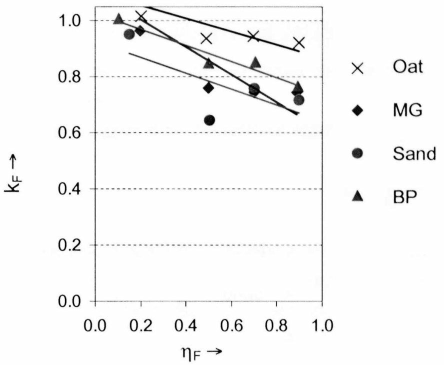

Fig. 4: Velocity coefficient k_F depending on fill ratio and sort bulk solid.

From the comparison of diagrams in Fig. 2 and 4 follows that the experimental results obtained by means of the pilot plant correspond with results of the test rig.

Additionally the analysis of diagrams in Fig. 1,2, and 4 also shows that the conveyance of oat is much better as mix granulate. The form of oat-grain, the one dimension of which is longer than two others, may explain this. Consequently the interlocking properties are better, which influence the straightforward component of bulk solid motion positively.
Experimental results for velocity coefficient k_F presented in Fig. 4 are summarised in form of regression equations in Tab. 1.

3 Experimental study of mechanical characteristics in HSSCs

The HSSC of the large-scale pilot plant is used to investigate the total torque and axial force in HSSCs. This involves the investigations in non-load and load operating modes. It helps to determine the coefficients of motion resistances for torque moment M_F and axial force F_{ax} depending on bulk solid and operating characteristics of HSSC. These coefficients are very important for design of HSSCs.

3.1 Non-load operating mode

Expectedly, the torque M_{W0} in non-load operating mode depends on wall friction coefficient μ_{FW} (remaining bulk solid/trough) and does not depend on rotational speed n_W (Fig. 5). That applies to the resulting fictive coefficient of motion resistance λ_0 (Eq. 26) from Part 1.

The fictive coefficient of motion resistance λ_0 of HSSCs may be calculated generally from Part 1 with Eq. (26) and (48):

$$\lambda_0 = k_W \cdot \cos\delta \cdot \mu_{FW} \,. \tag{1}$$

In particular case of HSSC ($\delta = 0°$) the Eq. (1) takes the form of:

$$\lambda_0 = k_W \cdot \mu_{FW} \tag{2}$$

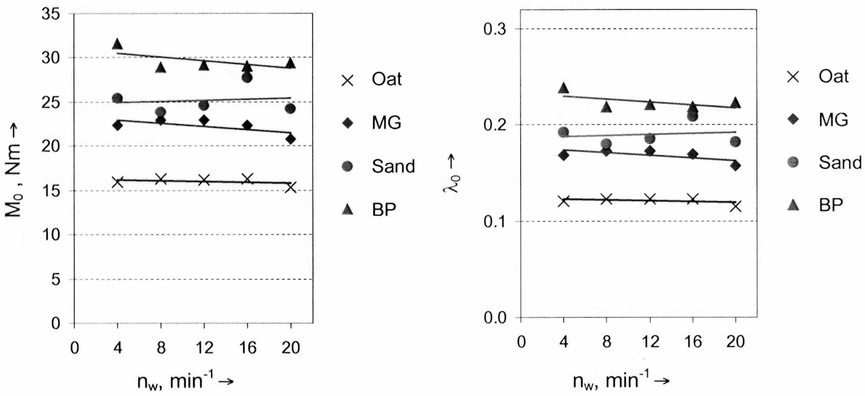

Fig. 5: Torque M_{W0} and fictive coefficient of motion resistance λ_0 in non-load operating mode depending on rotational speed n_W and sort of remaining bulk solid.

The mass coefficient k_W of shaftless screw shows what part of the screw is supported by the trough ($0 < k_W < 1$). The value of mass coefficient k_W depends on tolerances of conveyor's mechanical components and installation and may have different values for the same conveyor (e.g. before and after instalation of screw). Due to this it may in practice be assumed, that all mass of shaftless screw is supported by the trough. The mass coefficient is then $k_W \approx 1$. Hence the Eq. (2) takes the form of:

$$\lambda_0 = \mu_{FW} \,. \tag{3}$$

Thus the torque M_{W0} from Part 1 (Eq. 48) for HSSC is given by:

$$M_{W0} = M_{W0th} = m_W \cdot g \cdot \mu_{FW} \cdot r_{Wa} \tag{4}$$

The calculated value of torque with Eq. (4) M_{W0th} and measured value of torque in experiment M_{W0exp} with HSSC of pilot plant in non-load operating mode help to calculate the mass coefficient as its ratio. For the HSSC of pilot plant the mass coefficient k_W is within the interval $0{,}35 \leq k_W \leq 0{,}48$.

3.2 Load operating mode

The configuration of HSSC-VSSC-system is a very common practice. The same configuration is used in pilot plant described in this study in the article "Research on shaftless screw conveyors" (see above). In the operating of HSSC-VSSC-system the ratio of rotational speeds of HSSC and VSSC is very important to avoid the mechanical overloading on the intersection between the two conveyors.
The experiments with pilot plant shows that the ratio of rotational speeds has to be at least:

$$\frac{n_{Wv}}{n_{Wh}} > 1{,}5 \qquad (5)$$

Some companies design the HSSC-VSSC-systems, which have the diameter of VSSC greater than the HSSC. It helps not only to avoid the blockage on the intersection between two conveyors but also the repair of the system is easier in case of blockage.

In experiments the total axial force and the press force were measured. The difference between two values presets the axial force due to motion resistance in conveyor.

If the ratio of rotational speeds is chosen in consideration with Eq. (5) the press force may be neglected ($F_P \approx 0$).

Fig. 6 presents the general character of signal of the measured total torque in load operating mode by transport of mix granulate (l.) by fill ratio $\eta_F \approx 0{,}5$ and basalt powder (r.) by $\eta_F \approx 0{,}7$ with rotational speed n_W = 16 min^{-1}. The same signal character has the axial force on the screw.

In the case of oat, sand and mix granulate the signal oscillates at an average value. There is no start-up process in the signal. In contrast to this, the start-up process occurs in the signal of M_W and F_{ax} in the experiments with basalt powder. After finishing the start-up process in basalt powder the signal of M_W and F_{ax} decreases and oscillates at an average value too. Due to this, the total torque and axial force have to be calculated in consideration with start-up coefficient:

$$M_{an} = k_{an} \cdot M_W, \qquad (6)$$

and

$$F_{an} = k_{an} \cdot F_{Wax}. \qquad (7)$$

For the cohesive bulk solids the start-up coefficient k_{an} is:

$$k_{an} \approx (1{,}3 \ldots 1{,}5). \qquad (8)$$

For the grained free flowing bulk solids the start-up coefficient k_{an} may be estimated with:

$$k_{an} \approx 1{,}0 \qquad (9)$$

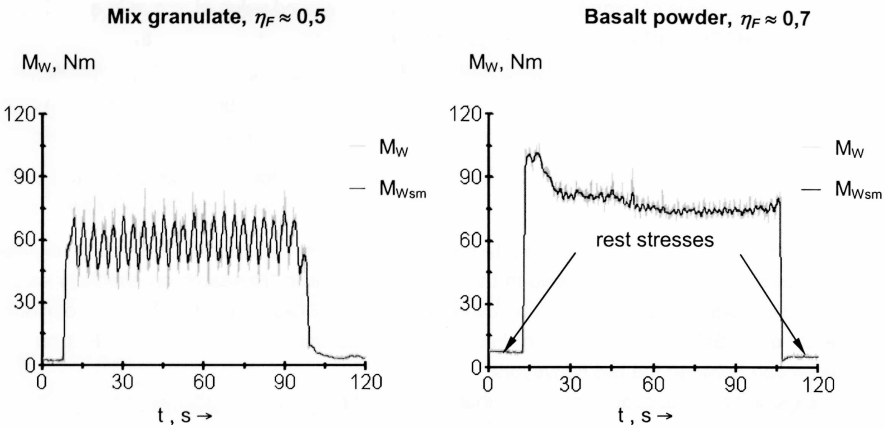

Fig. 6: Character of measured signal (original and smoothed) of total torque M_W by transport of mix granulate (l.) by $\eta_F \approx 0,5$ and basalt powder (r.) by $\eta_F \approx 0,7$ with $n_W = 16\ min^{-1}$

Figure 7 illustrate the results of the experiments, which are the torque moment M_F and the axial force F_{ax} due to motion resistance in HSSC depending on the fill ratio η_F, rotational speed n_W and the sort of bulk solid. The fictive coefficient of motion resistance λ_F and the specific power P_{spc} (Fig. 8) are calculated with Eq. (27) – (29) [Part 1] from known experimental values of torque M_F and mass productivity I_m.

Figures 7 and 8 show that the torque M_F , the axial force F_{ax} , the fictive coefficient of motion resistance λ_F and the specific power P_{spc} increase linearly with the increase of fill ratio η_F. The rise of characteristics on diagrams depends on bulk solid properties.

For grained bulk solids (oat, sand and mix granulate) the mechanical characteristics (M_F , F_{ax}, λ_F , P_{spz}) increase linearly with the increase of fill ratio η_F and do not depend on usual rotational speeds.

The mechanical characteristics (M_F , F_{ax}, λ_F , P_{spz}) for basalt powder increase more strongly depending on the fill ratio η_F by slower rotational speeds $n_W < 8\ min^{-1}$ than by higher ones $n_W \geq 8\ min^{-1}$ (Fig. 7, 8). This consideration may be applied to all cohesive powder bulk solids by its conveyance with fill ratio $\eta_F > 0,5$.

The reason for that is that the cohesive and adhesive properties of bulk solid influence the mechanical characteristics (M_F , F_{ax} , λ_F , P_{spz}) more strongly at low rotational speeds. In this case the motor has to overcome the high internal friction forces in bulk solid in addition to the wall friction forces between bulk solid and screw and trough.

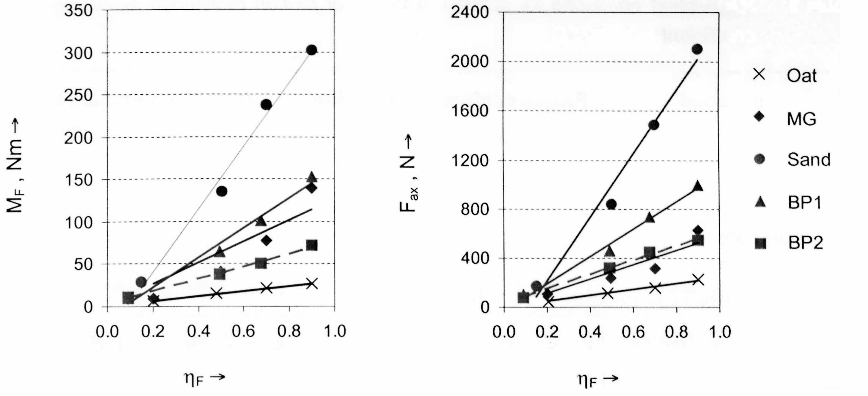

Fig. 7: Torque M_F (l.) and axial force F_{ax} (r.) due to motion resistance depending on fill ratio η_F and sort of bulk solid

It is necessary to mention that by low rotational speeds the bulk solid properties (which are determined in the lab) do not change during conveyance. By high rotational speeds the bulk solid properties are changed because of fluidization. Due to this the internal and wall friction, cohesion and adhesion of bulk solid decrease. Consequently the mechanical characteristics (M_W, F_{ax}, λ_F , P_{spz}) decrease too.

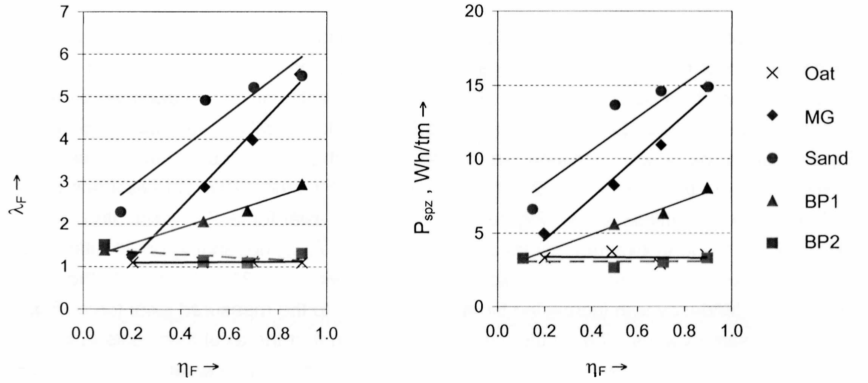

Fig. 8: Fictive coefficient of motion resistance λ_F (l.) und specific power P_{spc} (r.) depending on fill ratio η_F and sort of bulk solid

Important to emphasize, is that in this study, unchanged bulk solid properties are assumed. Due to this only the experimental results of basalt powder for n_w = 4 min^{-1} (*BM1*) will be analyzed. Though the manufacturer should use the diagrams of basalt powder for n_w = 8 ... 20 min^{-1} (*BM2*) to design the HSSCs-systems, because the conveyance by low rotational speeds is inefficient.

The results presented in Fig. 7 and 8 may be compiled in form of regression equations (Tab.1).

Table 1: Regression equations for fictive coefficient of motion resistance λ_F and velocity coefficient k_F in HSSC

Bulk solid	Fictive coefficient of motion resistance λ_F	Velocity coefficient k_F
Oat	$\lambda_F = 0{,}02 \cdot \eta_F + 1{,}1$	$k_F = -0{,}23 \cdot \eta_F + 1{,}1$
Mix granulate	$\lambda_F = 6{,}03 \cdot \eta_F - 0{,}02$	$k_F = -0{,}49 \cdot \eta_F + 1{,}1$
Fine-grained sand	$\lambda_F = 4{,}33 \cdot \eta_F + 2{,}05$	$k_F = -0{,}28 \cdot \eta_F + 0{,}93$
Basalt powder 1 (BP1), $n_W < 8$ min^{-1}	$\lambda_F = 1{,}85 \cdot \eta_F + 1{,}19$	$k_F = -0{,}29 \cdot \eta_F + 1{,}03$
Basalt powder 2 (BP2), $8 \leq n_W \leq 20$ min^{-1}	$\lambda_F = -0{,}32 \cdot \eta_F + 1{,}5$	$k_F = -0{,}29 \cdot \eta_F + 1{,}03$

4 Calibration of theoretical equations for calculation of mechanical characteristics for HSSCs

The 1st part of this article presents the simplified calculation model and the theoretical model for calculation of mechanical characteristics for HSSCs. The simplified calculation model is adapted for practical purposes by λ_0-, λ_F-, k_F-, k_δ-coefficients, which are obtained by means of experimental results. Only the Eq. (31) [Part 1] should be calibrated here. Originally the Eq. (31) gives the relation between turning torque and the axial force developed between a screw and nut of the drive screw [21], [24]. It is used in this study [Part 1] to estimate the axial force on the shaftless screw. Figure 9 illustrates the axial force F_{Sax} calculated with Eq. (31) by k_{ax} = 1 and in experiments measured axial force F_{axexp} depending on fill ratio η_F and sort of bulk solid. The axial force, which is calculated with Eq. (31), shows only the similar (increasing) tendency with increasing fill ratio comparing to the measured axial force (Fig. 9), but not the same values. The problem is the assumption that the axial force acts at the middle pitch of diameter. In reality the position of the acting point of the axial force depends on conveyor's parameters as well as on bulk solid. This is why this equation should be corrected to reality for SSCs by a factor k_{ax}:

$$k_{ax} = \frac{F_{ax\exp}}{F_{Sax}}. \qquad (10)$$

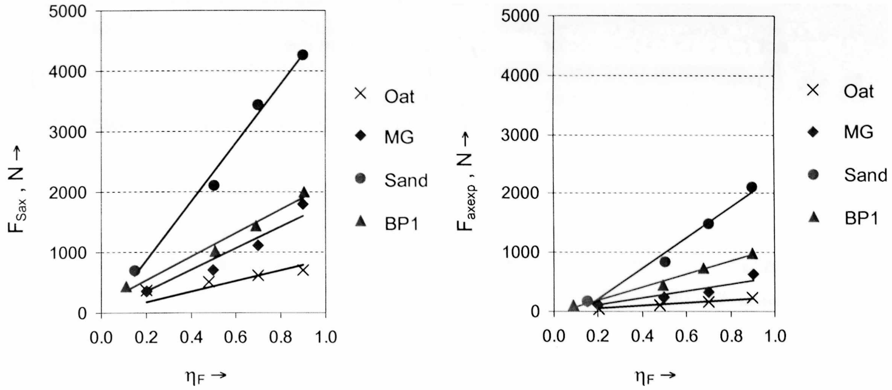

Fig. 9: The axial force F_{Sax} (l.) calculated with Eq. (31) (by k_{ax} = 1) and in experiments measured axial force F_{axexp} (r.) depending on fill ratio η_F and sort of bulk solid

Figure 10 illustrates the correction factor k_{ax} for axial force F_{axexp} depending on fill ratio η_F and the sort bulk of solid. It may be presented in form of regression equations (Tab.2).

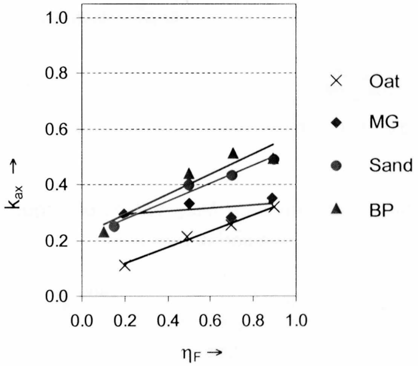

Fig. 10: The correction factor k_{ax} for axial force F_{Sax} depending on fill ratio η_F and bulk solids

Table 2: Regression equations for correction factor k_{ax} in HSSC.

Bulk solid	**Correction factor k_{ax}**
oat	$k_{ax} = 0{,}3 \cdot \eta_F + 0{,}06$
mix granulate	$k_{ax} = 0{,}06 \cdot \eta_F + 0{,}29$
fine-grained sand	$k_{ax} = 0{,}32 \cdot \eta_F + 0{,}22$
basalt powder	$k_{ax} = 0{,}36 \cdot \eta_F + 0{,}23$

In the practice the correction factor k_{ax} may be chosen from the interval:

$$k_{ax} = (0,2...0,5). \tag{11}$$

The greater values in Eq. (11) should be taken for problematic and heavy bulk solids, for high fill ratios and high angles of elevation.

The next step is adaptation of the theoretical model for HSSCs from Part 1 to practical use.

Figures 11 and 12 illustrate the torque and axial force in HSSC, whose values are calculated with equations from theoretical model (M_{Fth} , F_{axth}) and measured in experiments (M_{Fexp} , F_{axexp}) with pilot plant.

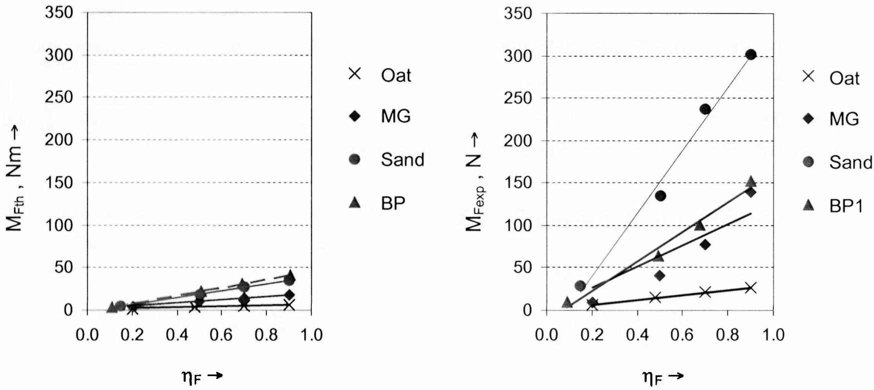

Fig. 11: Theoretical M_{Fth}, and measured M_{Fexp} values of torque due to friction of bulk solid depending on fill ratio η_F and sort of bulk solid

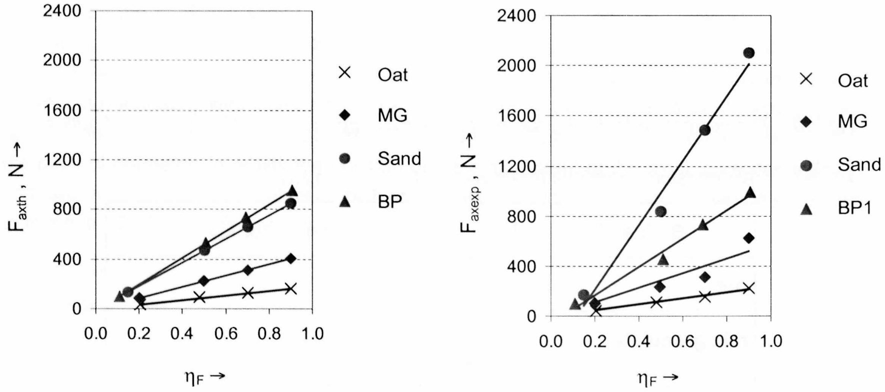

Fig. 12: Theoretical F_{axth}, and measured F_{axexp} values of axial force depending on fill ratio η_F and sort of bulk solid

The Figures 11 and 12 show that the theoretical torque M_{Fth} and axial force F_{axth} have only similar (increasing) tendency with increasing fill ratio comparing to the measured values.

It illustrates the complexity of M_F and F_{ax} dependency on bulk solid properties, fill ratio, geometry parameters of shaftless screw and in case of powder bulk solids on the rotational speed. In order to "calibrate" the theoretical model the calculative coefficients of motion resistances for torque moment λ^*_{MW} and axial force λ^*_{Fax} should be introduced. They consider the additional motion resistance, which cannot be calculated theoretically.

The calculative coefficients of motion resistances λ^*_{MW} and λ^*_{Fax} may be obtained by means of theoretically calculated M_{Fth} , F_{axth} and experimentally measured M_{Fexp} , F_{axexp} values of torque and axial force:

$$\lambda^*_{MW} = \frac{M_{F\,exp}}{M_{Fth}}, \tag{12}$$

and

$$\lambda^*_{Fax} = \frac{F_{ax\,exp}}{F_{axth}}. \tag{13}$$

Figure 13 illustrates the calculative coefficients of motion resistances for torque moment λ^*_{MW} and axial force λ^*_{Fax} depending on fill ratio η_F and sort of bulk solid. They are presented in form of regression equations in Tab. 3 as well.

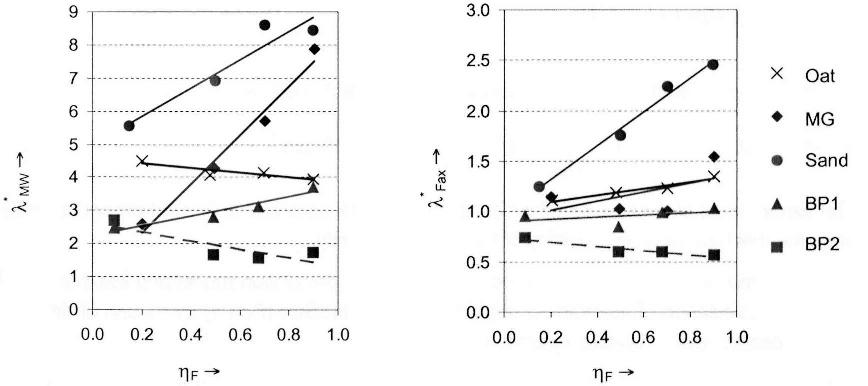

Fig. 13: The calculative coefficients of motion resistances for torque moment λ^*_{MW} and axial force λ^*_{Fax} in HSSC depending on fill ratio η_F and sort of bulk solid

Table 3: Regression equations for calculative coefficients of motion resistances λ^*_{MW} and λ^*_{Fax} in HSSC

Bulk solid	**Calculative coefficient of motion resistances for torque moment M_F** λ^*_{MW}	**Calculative coefficient of motion resistances for axial force F_{ax}** λ^*_{Fax}
Oat	$\lambda^*_{MW} = -0{,}71 \cdot \eta_F + 4{,}6$	$\lambda^*_{Fax} = 0{,}33 \cdot \eta_F + 1{,}1$
Mix granulate	$\lambda^*_{MW} = 7{,}4 \cdot \eta_F + 0{,}9$	$\lambda^*_{Fax} = 0{,}46 \cdot \eta_F + 0{,}92$
Fine-grained sand	$\lambda^*_{MW} = 4{,}25 \cdot \eta_F + 5$	$\lambda^*_{Fax} = 1{,}7 \cdot \eta_F + 1{,}0$
Basalt powder 1 (BP1), n_W < 8 min^{-1}	$\lambda^*_{MW} = 1{,}5 \cdot \eta_F + 2{,}25$	$\lambda^*_{Fax} = 0{,}12 \cdot \eta_F + 0{,}9$
Basalt powder 2 (BP2), 8 $\leq n_W \leq$ 20 min^{-1}	$\lambda^*_{MW} = -1{,}35 \cdot \eta_F + 2{,}7$	$\lambda^*_{Fax} = -0{,}21 \cdot \eta_F + 0{,}75$

5 Concluding remarks

The experimental study was accomplished for HSSCs with the typical parameters:

$k_r \approx 0{,}27...0{,}97$, $\delta = 0°...32°$, $\frac{l_{St}}{d_{Wa}} \approx 0{,}63...1{,}1$ und $n_W < 30$ min^{-1}.

The experiments also show that the operating characteristics and bulk solid properties influence the mechanical characteristics of HSSCs significantly.

The experimental results help to calibrate the simplified calculation model and the theoretical model for calculation of mechanical characteristics for HSSCs [Part 1] by means of different empiric coefficients for practical purposes.

Although the theoretical model better reflects the physical processes in the trough of HSSC, it does not have an important advantage compared to the simplified calculation model from the practical point-of-view of the industrial manufacturer. The theoretical model needs to be "calibrated" as well the simplified calculation model by empiric coefficients to get realistic calculation results.

All results of this study can be summarized in the following:

- The mechanical characteristics (M_F, F_{ax}, λ_F, P_{spz}) for grained bulk solids increase roughly linearly with the increase in fill ratio η_F. They do not depend on usual rotational speeds. The cohesive powder bulk solids increase more sharply depending on the fill ratio η_F by slower rotational speeds than by higher ones, because of fluidization. The fluidization occurs by higher rotational speeds and causes the changing of bulk solid properties.

- The fictive coefficient of motion resistance λ_F depends on fill ratio, bulk solid properties and, in case of powder bulk solids, on rotational speed too. It is located in an interval $1 < \lambda_F < 6$. For HSSCs by fill ratios $\eta_F \leq 0{,}3$ the λ_S -values from DIN 15262 [4] can be used.
- The velocity coefficient k_F in HSSC depends on fill ratio and bulk solid properties. It is located in an interval $0{,}6 < k_F < 1$. The velocity coefficient is $k_F \approx 1$ by $\eta_F < 0{,}3$.
- The velocity coefficient k_δ in HSSCs depends on fill ratio, angle of elevation and bulk solid properties. It is located in an interval $0{,}6 < k_\delta < 1$.
- The HSSCs works efficiently by fill ratios $0{,}5 \leq \eta_F \leq 0{,}9$ and low rotational speeds $8 \leq n_W < 30$ min^{-1}. The recommendations for choice of geometrical parameters for shaftless screw are mentioned in Part 1.

Nomenclature

A_F , A_T	conveyance and trough cross sectional area	m^2
F_F	weight of bulk solid in the trough	N
F_{R1}, F_{R2}	frictional forces between shaftless screw and masses of bulk solidsm_1, m_2	N
F_{RT}	total frictional force due to friction bulk solid/trough	N
F_{Sax}	axial force of the drive screw in consideration of a correction factor k_{ax}	N
F_{ax}	axial force acting on the shaftless screw (without press force F_p)	N
F_{ax1}, F_{ax2}	axial forces between shaftless screw and masses of bulk solid m_1, m_2	N
I_m, I_V	mass and volumetric throughput of conveyor	t/h , m^3/h
L_R	lever arm of forces F_{R1}, F_{R2}	m
L_T, L_W	length of trough and shaftless screw	m
M_F , P_F	total torque and conveyor power due to friction of bulk solid in conveyor	Nm, W
M_{FW} , P_{FW}	torque and power consumption due to the friction between bulk solid and screw	Nm, W
M_W, P_W	total torque and power of SSC	Nm, W
M_{W0}, P_0	total torque and power consumption in no-load operating mode	Nm, W
M_{an} , F_{an}	total torque and axial force in the moment of start-up mode	Nm, N
M_n , P_n	nominal torque and nominal power of drive	Nm, W
P_{St} , P_{spc}	elevation and specific power	W , W·s/kg·m
P_{ax}	power consumption due to the axial force acting on the shaftless screw	W
P_{spc}	specific conveyor power	W·s/kg·m
S_{res}	resulting center of gravity	
S_1, S_2	centers of gravity of mass parts m_1, m_2	
V_F, V_T	volume of bulk solid in trough and effective volume of trough	m^3
V_W	volume of shaftless screw	m^3
V_{Ring} , V_{Ww}	volume of the ring and of one shaftless screw coil	m^3
b_W , l_{St}	blade width and pitch	m
d_{TO}, d_{TU}	inner diameter of O- and U-section of trough	m
d_T, r_T	effective inner diameter and radius of trough	m
d_{Wa}, d_{Wm}, d_{Wi}	outside, mean and inner diameter of shaftless screw	m
k_F, $k_{F\delta}$, k_δ	coefficients for conveyance velocity (velocity coefficients)	
k_{an}	start-up coefficient	
k_{ax}, k_w	correction factor for F_{Sax} and mass coefficient of shaftless screw	
k_r	coefficient of radii ratio	
m	mass of bulk solid in the screw chamber	kg
m_1, m_2	masses of bulk solid in the screw chamber	kg
m_D	grain destruction mass	%
m_F, m_W	mass of bulk solid in conveyor and mass of shaftless screw	kg
$\overline{m}_W$	distributed mass of shaftless screw	kg/m
n_W , n_n	rotational speed and nominal rotational speed of shaftless screw	s^{-1}, min^{-1}
r_{Wa}, r_{Wm}, r_{Wi}	outside, mean and inner radius of shaftless screw	m
s_W , s_{Schl}	thickness of blade and of wear-resistant liner	m
t	time	s
v_F	conveyance velocity	m/s
v_{F0}, $v_{F\delta}$	conveyance velocities by the angle of elevation $\delta = 0$ and $\delta \neq 0$	m/s

v_W , v_u	axial velocity of the screw and screw velocity due to its rotation	m/s
y_{res0}, y_{res}	resulting ordinates of centre of gravity for cross section of bulk solid body in static and dynamic steady-state	
z_W	number of pitches of the shaftless screw	
α_{Schl}	angle of wear-resistant liner	rad, grad
α_a, α_m	helix angle of the screw flight corresponding to the outer and mean screw radius	rad, grad
α_R,	helix angle of screw flight corresponding to the screw radius $r_W = L_R$	rad, grad
β_1 , β_2	auxiliary angles	rad, grad
δ	angle of elevation	rad, grad
ϵ	offset angle or slope angle of surface	rad, grad
ϕ_{FW}	wall friction angle bulk solid/screw	rad, grad
η_F, η_{FR}	fill ratio and remaining fill ratio	
η_V	volumetric ratio	
λ_0, λ_F	fictive coefficient of motion resistance in no-load and load operation mode in HSSC	
λ_S	fictive coefficient of motion resistance in HSCs	
$\lambda^{\bullet}_{Mw}$, $\lambda^{\bullet}_{Fax}$	calculative coefficients of motion resistances for torque moment M_F and axial force F_{ax}	
μ_{FT}, μ_{FW}, μ_{WT}	wall friction coefficients bulk solid/trough, bulk solid/screw and screw/trough	
ρ_b	bulk density	kg/m^3
ω_W	angular velocity of shaftless screw	s^{-1}

Abbreviations and Indices

HSC	horizontal screw conveyor
HSCs	horizontal and lightly inclined (until $\delta \leq 20°$) screw conveyor(s)
HSSC	horizontal shaftless screw conveyor
HSSCs	horizontal and lightly inclined shaftless screw conveyor(s)
STF, TF, UTF	sub-transitional, transitional and upper-transitional elevation field
VSSC	vertical shaftless screw conveyor
VSC	vertical screw conveyor
VSCs	vertical and steeply inclined screw conveyors
VSSCs	vertical and steeply inclined shaftless screw conveyors
cr	critical
tot	total
a, m, i	outer-, middle-, inner-
exp, th	experimental or theoretical
sm	smoothed

Literature

[1] Böttcher, S.: Eine allgemeine Analyse der Aufwärtsförderung eines Einzelkörpers in Schneckenförderern beliebiger Neigung. Teil 1bis 3. VDI-Zeitschrift 105 (1963) Nr. 14, S. 581-593; Nr. 16, S. 663-671; Nr. 18, S. 743-754.

[2] Bruck, R.: Conveying and compacting apparatus having a shaftless spiral in a casting with drainage openings, Patent US 005 562 029 A, 08.10.1996

[3] Bruck, R.: Parameter und Einsatzbereiche von Spiralförderern. Fachtagung Schüttgutfördertechnik 1998 - Tagungsband, Magdeburg, Otto-von-Guericke-Universität 1998

[4] DIN 15262 Januar 1983: Schneckenförderer für Schüttgut – Berechnungsgrundsätze (January 1983 „Screw conveyor for bulk solid – Basic principles of calculation")

[5] Ephremidis, C.: Untersuchungen zum Fördervorgang beim waagerechten Schneckenförderer. Hannover, Technische Universität, Diss. 1957

[6] Günthner, W.; Fottner, J.; Rong, O.: Empirische Entwicklung von Kenngrößen zur Auslegung von Hochleistungs-Schneckenförderern für Schüttgut. AiF-Forschungsbericht, TU München, FML, 2002

[7] Grigorjev, A.: Schneckenförderer. Moskau: Maschinostroenie, 1972.

[8] Kessler, F.; Leitner, J.; Lichtenecker E.: Calculation of fill ratio and mass flow rate of the vertical screw conveyor. Bulk solid handling, vol.22, No.3, pp. 190-220, 2002

[9] Krause, F.: Einsatz eines Wendelförderersystems (Spiralfördersystems) für Rohbraunkohle-Mischbrennstoff. Unveröffentl. Gutachten, Magdeburg, Otto-von-Guericke Universität, 2002.

[10] Krause, F.; Rodenbeck, A.W.; Haase, H.; Minkin, A.: Planung von Wendelförderern in der Verfahrenstechnik. Fachtagung Schüttgutfördertechnik 2000 – Tagungsband, Technische Universität München

[11] Krause, F.; Minkin, A.: Theoretical and experimental research on shaftless screw conveyors. The 4th International Conference for Conveying and Handling of Particulate Solids, Budapest 2003.

[12] Krause, F.; Banse, W.; Minkin, A.: Auslegung eines reversierbaren horizontalen Wendelförderers für Gips mit Restfeuchte. Unveröffentl. Forschungsbericht, Magdeburg, Otto-von-Guericke Universität, 2003.

[13] Minkin, A.: Funktionsanalyse von Wendelförderern. Magdeburg, Otto-von-Guericke Universität, Diss. 2005

[14] Pajer, G.; Kuhnt, H.; Kurth, F.: Lehrbuch Stetigförderer, 4. Auflage, VEB Verlag Technik Berlin, 1983.

[15] Preobrazensky; Trufanow: Biegsamer Wendelförderer und Mischer. KHTI, Kazan, 1970.

[16] Rodenbeck, A. W.: Handbuch zur Auslegung von Spiralfördersystemen. ImRo Bückeburg, 1997

[17] Rodenbeck, A. W., Kroos H.: Vorrichtung und Verfahren zum Austragen von Feststoffen aus einem Feststoff-Flüssigkeits-Gemisch, Patent DE 197 58 038 A1, 01.07.1999

[18] Rodenbeck, A. W., Kroos H.: Vorrichtung und Verfahren zum Fördern von Materialien, Patent DE 197 58 039 A1, 01.07.1999

[19] Rong, O.: Auslegungsverfahren für Hochleistungs-Schneckenförderern. TU München, Diss. 2004

[20] Roberts, A.: Design and Performance Criteria for Screw Conveyors in Bulk Solids Operation, Centre for Bulk Solids and Particulate Technologies, The University of Newcastle, Australia

[21] Rogler E.; Krauß, H.: Fördertechnik/Schneckenförderer, Fachhochschule Wiesbaden und Darmstadt.

[22] Sinha, G. L.: Untersuchungen zum Fördervorgang beim senkrechten Schneckenförderer. Hannover, Technische Universität, Diss. 1959

[23] Schulze, D.; Schwedes, J.: Der Fördervorgang in biegsamen Schneckenförderern. Fördern und Heben, Mainz 39 (1989) 3, S. 231 – 235

[24] Spivakovskij A.; Diatschkov, V.: Förderanlagen, Berlin: VEB Verlag Technik 1959.